A PRELIMINARY STUDY OF THE DISPLACEMENT OF SULPHITE BY TETRAPHENYLBORATE ON TRITYL DERIVATIVES

STEPHEN JOHN COLLENS


CENTRE FOR NFLD. STUDIES
OCT 6 1981
MEMORIAL UNIVERSITY
OF NEWFOUNDLAND

NOTICE

The quality of this microfiche is heavily dependent upon the quality of the original thesis submitted for microfilming. Every effort has been made to ensure the highest quality of reproduction possible.

If pages are missing, contact the university which granted the degree.

Some pages may have indistinct print especially if the original pages were typed with a poor typewriter ribbon or if the university sent us a poor photocopy.

Previously copyrighted materials (journal articles, published tests, etc.) are not filmed.

Reproduction in full or in part of this film is governed by the Canadian Copyright Act, R.S.C. 1970, c. C-30. Please read the authorization forms which accompany this thesis.

THIS DISSERTATION HAS BEEN MICROFILMED EXACTLY AS RECEIVED

AVIS

La qualité de cette microfiche dépend grandement de la qualité de la thèse soumise au microfilmage. Nous avons tout fait pour assurer une qualité supérieure de reproduction.

S'il manque des pages, veuillez communiquer avec l'université qui a conféré le grade.

La qualité d'impression de certaines pages peut laisser à désirer, surtout si les pages originales ont été dactylographiées à l'aide d'un ruban usé ou si l'université nous a fait parvenir une photocopie de mauvaise qualité.

Les documents qui font déjà l'objet d'un droit d'auteur (articles de revue, examens publiés, etc.) ne sont pas microfilmés.

La reproduction, même partielle, de ce microfilm est soumise à la Loi canadienne sur le droit d'auteur, SRC 1970, c. C-30. Veuillez prendre connaissance des formules d'autorisation qui accompagnent cette thèse.

LA THÈSE A ÉTÉ MICROFILMÉE TELLE QUE NOUS L'AVONS REÇUE

A PRELIMINARY STUDY OF THE DISPLACEMENT OF SULPHITE BY TETRAPHENYLBORATE ON TRITYL DERIVATIVES

by

©Stephen John Collens, B.Sc.(Hon.)

A Thesis submitted in partial fulfillment
of the requirements for the degree of
Master of Science

Department of Chemistry
Memorial University of Newfoundland

July 1980

St. John's Newfoundland

Abstract

Nucleophilic substitution is and has been an active area of investigation for physical organic chemists. Ingold's original mechanistic descriptions, S_N1 and S_N2, were initially controversial because of the proposal of ionic intermediates in the S_N1 process. Now the controversy is over the lack of intermediates in the S_N2 process. Winstein proposed that the S_N1 ionization is better described in a stepwise fashion with the substrate forming first an intimate ion-pair with no solvent separation followed by ion-pairs succesively separated by layers of solvent until the kinetically free ions are obtained. Sneen extended this idea and claims that all substrates in nucleophilic substitution reactions ionize at least to the intimate ion-pair stage before nucleophilic attack. Thus, Sneen maintains that S_N1 and S_N2 are operationally equivalent to two extremes of a common mechanism through which all nucleophilic substitution reactions proceed. Sneen's proposal is criticized due to the difficulty in establishing the existence of the intimate ion-pair in reactions which display S_N2 kinetics.

The present study is concerned with the displacement of sulphite ion by tetraphenylborate ion on two trityl derivatives, namely malachite green and paramethoxymalachite green, using water as the solvent. A mechanistic description is derived, using spectrophotometric methods, which must include two different ionized forms of the substrate (differ-

ing by amount of solvent separation) which suggests that the Winstein ionization scheme is followed. Also, this reaction provides a method of measuring the rate of solvolysis of the sulphite ion from these trityl derivatives which has not been done before.

Acknowledgements

The author wishes to express his sincere thanks to Dr. J. M. W. Scott whose supervision made this thesis possible. The author also wishes to express his gratitude to Drs. P.D. Golding and A. R. Stein for their general encouragement and hints. Mr. Fred Steele was also very helpful in the setting up of the experimental equipment. Thanks are also due to Mr. Craig McNamara of ETV for his help in producing a final copy and to Mrs. Chiung-Chu Chen for drafting the graphs. Financial assistance in the forms of a Graduate Scholarship from the Natural Sciences and Engineering Research Council and a demonstratorship from the University are greatly appreciated.

Table of Contents

List of Tables

List of Figures

Introduction

Nucleophilic substitution reactions have been of great interest to physical organic chemists for many years. The early mechanisms postulated for nucleophilic substitution reactions were those proposed by Ingold: S_N1 and S_N2 (1), Schemes I and II respectively.

Scheme I

$$RX \rightleftharpoons R^{\oplus} + X^{\ominus}$$

$$R^{\oplus} + N^{\ominus} \longrightarrow RN$$

Scheme II

$$RX + N^{\ominus} \rightleftharpoons [N\cdots R\cdots X]^{\ominus} \longrightarrow RN + X^{\ominus}$$

In the S_N1 scheme, the rate determining step is the formation of the carbonium ion intermediate, followed by fast nucleophilic attack. Thus, the S_N1 scheme gives an observed rate which is independent of the nucleophile concentration and in the case of optically active centres of attack, racemization occurs. For the S_N2 scheme, the observed rate is dependent on the nucleophile concentration and optical inversion occurs at the centre of attack.

The original proposal of ionic intermediates in an organic reaction met with criticism (2); however, ionic intermediates in this reaction are now well established and attention has recently been focused on the possibility of intermediates in typical S_N2 processes. Also, some nucleophilic substitution reactions seem to display characteris-

tics in between the extreme S_N1 and S_N2 categories and these await satisfactory explanation (3, 4).

The present state of the debate over nucleophilic substitution mechanisms originates with Winstein (5-7) who proposed that in media of low dielectric constant (e.g. acetic acid) the S_N1 ionization is better described by a series of equilibria,

Scheme III

$$RX \rightleftharpoons R^{\oplus}X^{\ominus} \rightleftharpoons R^{\oplus}|X^{\ominus} \rightleftharpoons R^{\oplus}||X^{\ominus} \rightleftharpoons \ldots \rightleftharpoons R^{\oplus} + X^{\ominus}$$

in which the kinetically free ions are generated via the formation of ion-pairs of varying degrees of tightness and solvent separation. The possibility of nucleophilic attack on any or all of the Winstein intermediates must now be considered in any comprehensive description of nucleophilic substitution reactions. The importance of this scheme is the de-emphasis of major one step reactions and replacing them with more elaborate schemes which achieve the same results via a series of smaller steps (8).

The question now arises as to the influence of the stability of the carbonium ion on the numerous kinetic possibilities associated with Scheme III. If nucleophiles are capable of attacking any of the ionic intermediates and the neutral substrate, then the less stable carbonium ions will probably manifest less solvent separation before nucleophilic attack.

This mechanistic description led Sneen to propose the ion-pair theory (9-11) in which the substrate always ionizes at least to the intimate ion-pair stage before nucleophilic attack can occur,

Scheme IV

$$RX \underset{k_{-1}}{\overset{k_1}{\rightleftharpoons}} R^{\oplus}X^{\ominus}$$

$$R^{\oplus}X^{\ominus} + N^{\ominus} \xrightarrow{k_2} RN + X^{\ominus}$$

If the nucleophile concentration is in great excess over the substrate concentration, pseudo-first order kinetics will be followed, giving

$$[1] \qquad k_{obs} = \frac{k_1 k_2 [N^{\ominus}]}{k_{-1} + k_2 [N^{\ominus}]}$$

for the observed rate constant. If $k_{-1} >> k_2[N^{\ominus}]$ then Equation [1] simplifies to an expression which is linearly dependent on the nucleophile concentration. This extreme of Scheme IV is operationally equivalent to, but not the same as, the classical S_N2 reaction. This scheme also predicts optical inversion at the centre of attack since the nucleophile must approach the substrate on the opposite side from which the leaving group departs. The other extreme related to Equation [1] is established when $k_{-1} << k_2[N^{\ominus}]$. Under this condition, the rate becomes independent of nucleophile concentration, giving apparently S_N1 type kinetics, but ac-

companied by full inversion at the centre of attack. However, if k_{-1} is small, the reaction may involve further intermediates related to the Winstein ionization scheme leading to more highly solvent separated ion-pairs. Thus, both sides of the intermediate carbonium ion become more equally available to nucleophilic attack, which, in turn, leads to a higher degree of racemization. Therefore, Sneen (9) proposed that the observed kinetics of S_N1 and S_N2 are actually extremes of a common mechanism through which all nucleophilic substitution reactions proceed. Also, this common mechanism provides an explanation for intermediate reactions that are between S_N1 and S_N2 in order. However, this scheme has received much criticism (2) due to the difficulty in establishing the existence of the intimate ion-pair intermediate in reactions previously considered to follow S_N2 kinetics.

Because of the Sneen proposal, the structures and reactivities of carbonium ions have become much more important. For instance, trityl carbonium ions* have been used as model systems for the methyl carbonium ion (12, 13), but this model has met with severe criticism (2). LaMer (14) proposed that the trityl ion reactions were simple cation-anion combinations and this idea persists. The purpose of this thesis is to provide evidence that the mechanism for the cation-anion combination reactions in solution is prob-

---

*The term 'trityl ions' refers to any derivative of the trityl (triphenylmethyl) ion.

ably more complex.

Linear Free Energy Relationships

The introduction of three pertinent linear free energy relationships (LFER's) is useful at this point. These are the Swain-Scott LFER (15), the Brönsted LFER (16) and the Ritchie LFER (17). All of these LFER's are concerned with reactions following second order kinetics. The Swain-Scott LFER deals with reactions which display classic S_N2 kinetics. The Brönsted LFER deals with the effects of basicity on a substitution reaction. Finally, the Ritchie LFER deals with nucleophilic attack on stable carbonium ions, particularly the trityl ions.

The general equation for the Swain-Scott LFER is given by

$$[2] \quad \log\left(\frac{k}{k_o}\right) = sn$$

for reactions taking place in the same solvent, typically water. The parameter 's' is a measure of the sensitivity (selectivity) of the substrate to changes in 'n'. The parameter 'n' is a measure of the nucleophilicity of the substituting reagent.

Equation [2] requires a standard reaction for which the rate constant is k_o. The 's' and 'n' values are defined for this reaction. The standard reaction for the Swain-Scott LFER is the attack of water (solvent) on methyl bromide.

Methyl bromide is defined to have s = 1 with n = 0 for water. The value of 'n' for any nucleophile can be obtained by measuring the rate of reaction with methyl bromide and calculating 'n' from Equation [2]. Once the 'n' values for a series of nucleophiles have been determined, 's' values for other substrates can be obtained from their rates of reaction with the same series of nucleophiles.

The Brönsted LFER deals with the reactions of bases with substrates and is used here by assuming nucleophilicity and basicity are related quantities. The Brönsted LFER is given by

$$[3] \qquad k_2 = GK_b^{\beta}$$

where k_2 is the second order rate constant and K_b is the base equilibrium constant of the nucleophile. The G parameter is constant for a series of bases of similar structure. Under this restriction, nucleophilicity and basicity are probably closely related quantities. The β parameter is substrate dependent. If the substrate is a strong acid, then k_2 will depend less on K_b and β will be close to zero. In this case, the activated complex is said to be 'reactant like'. If the substrate is a weak acid, then k_2 will depend to a greater extent on K_b and β will be close to unity. In this case, the activated complex is said to be 'product like'. This correlation between β and reaction rates is equivalent to a restatement of the Hammond postulate (18).

By a simple manipulation of Equation [3],

[4] $$\log k_2 = c - \beta pK_b = c' + \beta pK_a$$

can be obtained. Therefore, a plot of log k_2 as a function of the pK_a of the nucleophiles should be linear with slope β. This LFER was originally devised in relation to the Brönsted definition of acids and bases (proton transfer reactions) but is also applicable to the more general Lewis definition. The Brönsted LFER also is relevant to the reactions of trityl ions with nucleophiles since trityl ions are Lewis acids and nucleophiles are Lewis bases. This LFER is, in effect, a measure of the reactivity of the system (log k_2) as a function of the reactivity of the nucleophile (pK_a). As already mentioned, slow reactions should show a strong dependence on pK_a (i.e. β close to unity) while fast reactions should show a lower dependence on pK_a (i.e. β closer to zero). This is borne out in observation. Bruice (19) has reported a β value for 0.41 for malachite green while I (20) have reported a β value of 0.52 for crystal violet. These β values are as expected since the reaction rates for malachite green are faster than the corresponding rates for crystal violet, as implied by their respective structures.

The Ritchie LFER is the most interesting correlation related to the study of trityl ions and is given by

[5] $$\log\left(\frac{k}{k_o}\right) = N^+$$

The standard reaction, for which k_o is the rate constant, is that between malachite green and water (solvent) with the N^+ value for this reaction defined as zero. The N^+ parameter is dependent on the nucleophile and is independent of the substrate.

The Ritchie LFER is of particular interest because there is no selectivity parameter which depends on the substrate (c.f. Equation [2]). Equation [5] does not appear to be universally valid. Thus Scott and co-workers (21) report the reaction rate constants of tris-p-anisylmethyl cation with a series of nucleophiles and compared these to the corresponding reaction rate constants for malachite green. This work provided an excellent linear correlation between the two series but the slope was not unity, as required by the Ritchie LFER. Therefore, Scott proposed a modification of the Ritchie LFER,

$$[6] \qquad \log\left(\frac{k}{k_o}\right) = S^+N^+$$

which includes a substrate dependent parameter, S^+.

Unquestionably, the Ritchie LFER provides an adequate fit for a wide variety of nucleophiles on a number of different substrates.* Nevertheless, the lack of a selectivity parameter tends to contradict the Hammond postulate. Ritchie claims that the lack of a selectivity parameter is simply

---

*A close inspection of the literature data from a variety of sources shows an alarming number of discrepancies.

that the reaction rate is primarily dependent on desolvation of the nucleophile (17). This claim is not supported by the β values of the Brönsted LFER for trityl ions since the β values do not indicate the activated complex to be as 'product like' as it should be. Pross proposes an argument (22) based on the solvation of the trityl ion to reconcile the Ritchie LFER with the Hammond postulate.

Pross' analysis of the situation is complex but his conclusions are easily summarized. In an aprotic solvent, the nucleophilicities of the halides are well known to be $F^{\ominus} > Cl^{\ominus} > Br^{\ominus} > I^{\ominus}$. However, in protic solvents, this order is reversed. This reversal is due to solvation phenomena. Because of the greater inherent nucleophilicity of $F^{\ominus}$ over $Cl^{\ominus}$, $F^{\ominus}$ is solvated by a protic solvent much more so than $Cl^{\ominus}$. This solvent interaction thus reduces the apparent nucleophilicity of $F^{\ominus}$ to less than that of $Cl^{\ominus}$.

The trityl ions also interact strongly with solvents capable of electron donation, of which water is an example. The extinction coefficients of the trityl ions are strongly dependent on solvent (23). The more capable the solvent is of donating electrons, the lower the extinction coefficient is. This observation indicates a stronger solvent-solute interaction with the more electron donating solvents. A logical deduction is to conclude that the more capable a trityl ion is of accepting electrons (i.e. the more reactive the trityl ion is), the better solvated it will be in a

basic solvent such as water.

The importance of the solvation of the trityl ions forms the gist of the Pross rationalization of the absence of a selectivity parameter in Equation [5] i.e. the more reactive the trityl ion is inherently, the better solvated it is in water. The better solvated the ion is, then the more its reactivity is decreased and hence its selectivity is increased. Thus, a trityl ion with inherently low selectivity will have its selectivity increased by solvation. These opposing effects apparently cancel, leading to the Ritchie LFER, in which most of the carbonium ions are embraced by an equation with no selectivity parameter.

Current Topic

The quantitative experiments reported in this thesis relate to a novel reaction. When the sulphite ion is added to a solution of malachite green (a trityl ion) chloride, the colour fades very rapidly, indicating covalent bond formation between the malachite green ion and sulphite ion. When sodium tetraphenylborate is added to this solution, a colour returns to the solution. This colour is the same as the colour of a malachite green solution with sodium tetraphenylborate added directly to it. Therefore, in aqueous solution, a species incapable of forming a covalent bond, tetraphenylborate ion, is capable of 'displacing' a covalently bonded species, sulphite ion.

Another interesting preliminary observation is the effect of solvent composition on this reaction. First, an aqueous solution of malachite green chloride is prepared with sodium sulphite added. This colourless solution is then diluted with acetone and remains colourless. When sodium tetraphenylborate is now added to this solution, the solution still remains colourless. This observation suggests that the displacement of sulphite by tetraphenylborate in aqueous solution is strongly influenced by solvation. In water, sulphite is probably better solvated than tetraphenylborate with a reversal of these conditions when acetone is added. The fact that tetraphenylborate is poorly solvated in water is demonstrated by the precipitation of potassium ions from water by the tetraphenylborate ion (24).

The displacement of sulphite ion by tetraphenylborate ion on a trityl ion is interesting for a number of reasons. This reaction is a 'nucleophilic' (for want of a better term) substitution in which the carbonium ion intermediate should be relatively stable. The leaving group, sulphite, is itself a very powerful nucleophile (21). The product must be an ionic species since it is coloured and tetraphenylborate ion is incapable of covalent bond formation. Also, this reaction provides a means for determining the rate of dissociation of sulphite ion from the trityl ions which may give some insight concerning the details of the reverse reaction, i.e. attack of sulphite on the trityl ions. In this sense,

the tetraphenylborate ion is a trap for the carbonium ions produced by the solvolysis of the tertiary sulphite. The solvolysis of tertiary compounds in water is itself an interesting area which because of the high reactivity of such compounds has generally been impossible to study.

Experimental

Materials

The chemicals used were paramethoxymalachite green perchlorate ($pMeOMGClO_4$), bis-(4-N,N-dimethylaminophenyl)-4-methoxyphenylmethyl perchlorate; malachite green chloride (MGCl), bis-(4-N,N-dimethylaminophenyl)-phenylmethyl chloride; sodium tetraphenylborate (NaTPB); sodium sulphite and quinol. The $pMeOMGClO_4$ was prepared and purified previously in this laboratory. The MGCl was Matheson, Coleman and Bell dye recrystallized from distilled water. The sodium sulphite was 'Baker Analyzed' reagent (100.0% assay). The NaTPB was Aldrich 'Gold Label' reagent (99+%) and the quinol was British Drug House reagent (99-101%). All solutions were made using freshly distilled water.

Measurements

The reactions were followed spectrophotometrically on a Pye Unicam SP500 equipped with cell jackets. Reactions involving $pMeOMG^{\bullet}$ and $MG^{\bullet}$ were followed at 602nm and 615nm respectively. All weighings were made on a four decimal place Mettler balance. The temperature was measured by a Hewlett-Packard 2801A quartz thermometer and maintained at 25.00 ± 0.05°C by a Neslab RTE-8 refrigerated circulating bath. All volumetric pipettes and flasks used were grade A quality. The cuvettes used were 1.00cm quartz cells and were rinsed with analytical grade acetone between runs.

Preparation of Solutions

The dye stock solutions were prepared by dissolving 0.2028g of MGCl in 1000.00ml water (5.557×10^{-4}M) and 0.1079g of pMeOMGClO$_4$ in 500.00ml water (4.692×10^{-4}M). The NaTPB stock solutions were made by weighing out the appropriate amount to make approximately 4.5×10^{-3}M in 500.00ml. The quinol stock was prepared by weighing out 0.1101g to make 1000.00ml of 1.00×10^{-3}M solution. This solution was then diluted 10.00ml in 100.00ml to give a stock of 1.00×10^{-4}M quinol. The NaTPB and quinol stocks were used within four days of preparation.

Kinetic Runs

All runs were prepared in 100.00ml volumetric flasks. The appropriate amounts of Na_2SO_3 were preweighed and placed in dry flasks. Each solution was then prepared from the dry Na_2SO_3 immediately prior to use. First, 1.00ml of the quinol stock was added, followed by 3.00ml of the dye stock. Next, the appropriate amount of NaTPB stock was added and the solution brought up to 100.00ml with water and thermostatted. The solutions now contain working concentrations of 1.00×10^{-6}M quinol and 1.667×10^{-5}M $MGSO_3^{\theta}$ or 1.408×10^{-5}M pMeO-$MGSO_3^{\theta}$. (The dyes are effectively transformed into their sulphites at these concentrations.) The quinol was added to stabilize the sulphite ion and did not affect the rates (17). The TPB^{θ} and $SO_3^{2\theta}$ concentrations were in a fair excess over

the dye concentrations and so were effectively constant.

In these runs, the solution started colourless and the rate of the return of colour was observed. For all of the runs, the infinity absorbance values were effectively constant for each dye. However, the infinity absorbances for the lowest TPB^{θ} concentrations on the $MGSO_3^{-\theta}$ runs were slightly lower.

Another noteworthy observation was the slow fading of the coloured product solution. The solutions took about a day to fade noticeably and were almost colourless after a few days. However, in the absence of light, the colour persisted for a much longer period of time, indicating a slow secondary photochemical reaction.

Analysis of Results

Kinetic data were initially analyzed using the three parameter curve fit based on the method by Moore (25) and described by Scott (26). This analysis gave a satisfactory result for the infinity absorbance value, but, for reasons to be discussed later, a poor fit of the data in terms of producing a pseudo-first order rate constant.

The infinity values obtained by the Moore method were used to fit the raw data to

$$[7] \quad \ln(P_i - P) = -k_{obs}\, t$$

and the value of k_{obs}, the pseudo-first order rate constant,

was determined by linear least squares. P_i is the infinity absorbance; P is the absorbance at time t. Usually, the first point or two of the run had to be dropped to obtain the best fit. These points were always deviating to give a lower value of k_{obs} when included. The justification for dropping these points is contained within the suggested schemes to represent the mechanism. All suggested schemes are multi-step and the initial points may deviate as observed due to the time of the induction period for steady state to be achieved and, once achieved, adherence to pseudo-first order kinetics.

Finally, the data were fitted to the devised rate law and the parameters were determined by an algorithm suggested by Wentworth (27) for general regression analysis. This method produced the best values of the parameters and calculated the standard deviations of each along with the covariances between the parameters. Guess values for the parameters were obtained from the linear least squares treatment of the data for the plots of k_{obs}^{-1} as a function of $SO_3^{2\Theta}$ concentration and slopes of these plots as a function of reciprocal TPB^{Θ} concentration. The errors used for k_{obs} were calculated from the raw data and the errors used for the concentration terms were ±5 in the last decimal place cited.

DATA

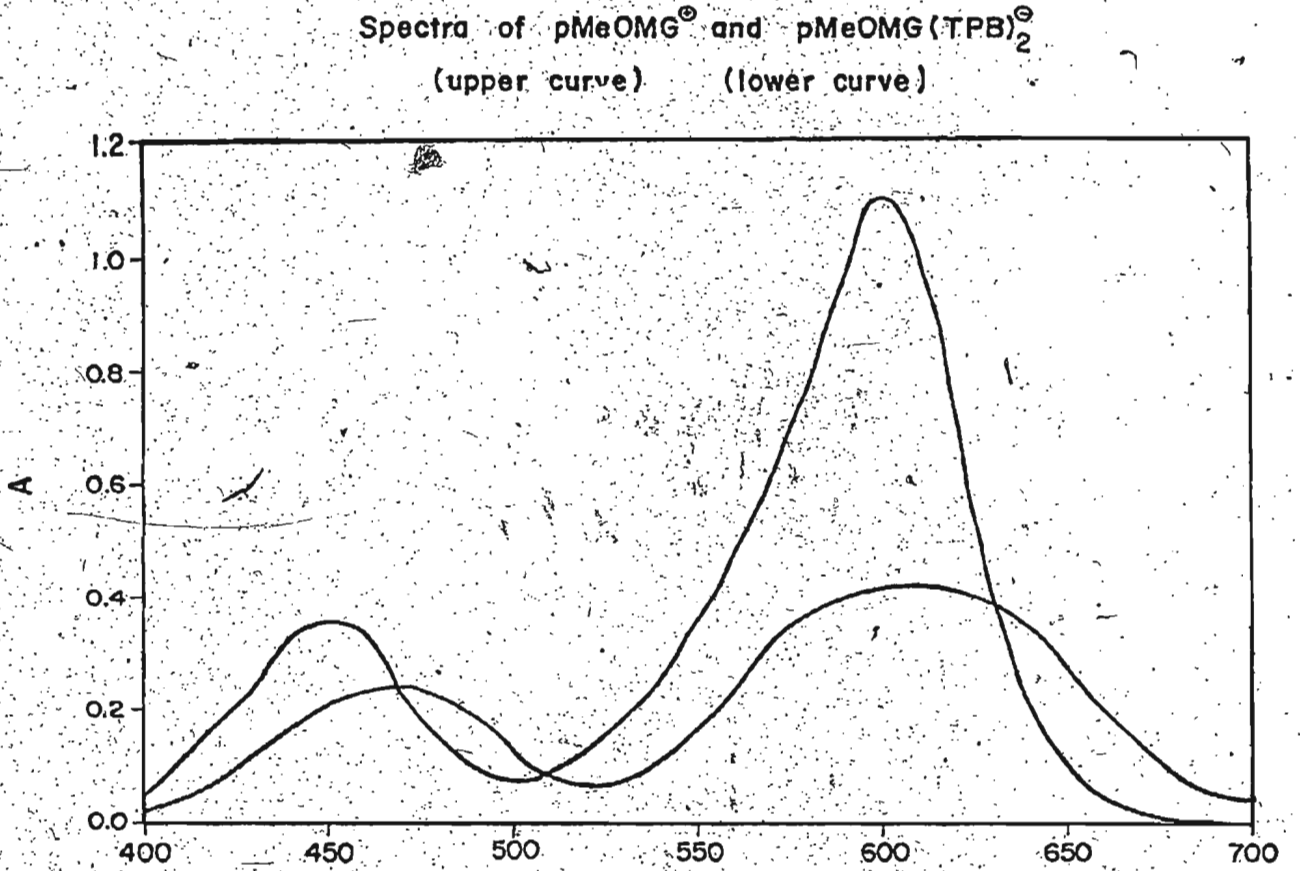
Spectra of pMeOMG⊕ and pMeOMG(TPB)⊖2
(upper curve) (lower curve)
1.2
1.0
0.8
0.6
0.4
0.2
0.0
A
400
450
500
550
600
650
700
λ (nm)

Fig. 1

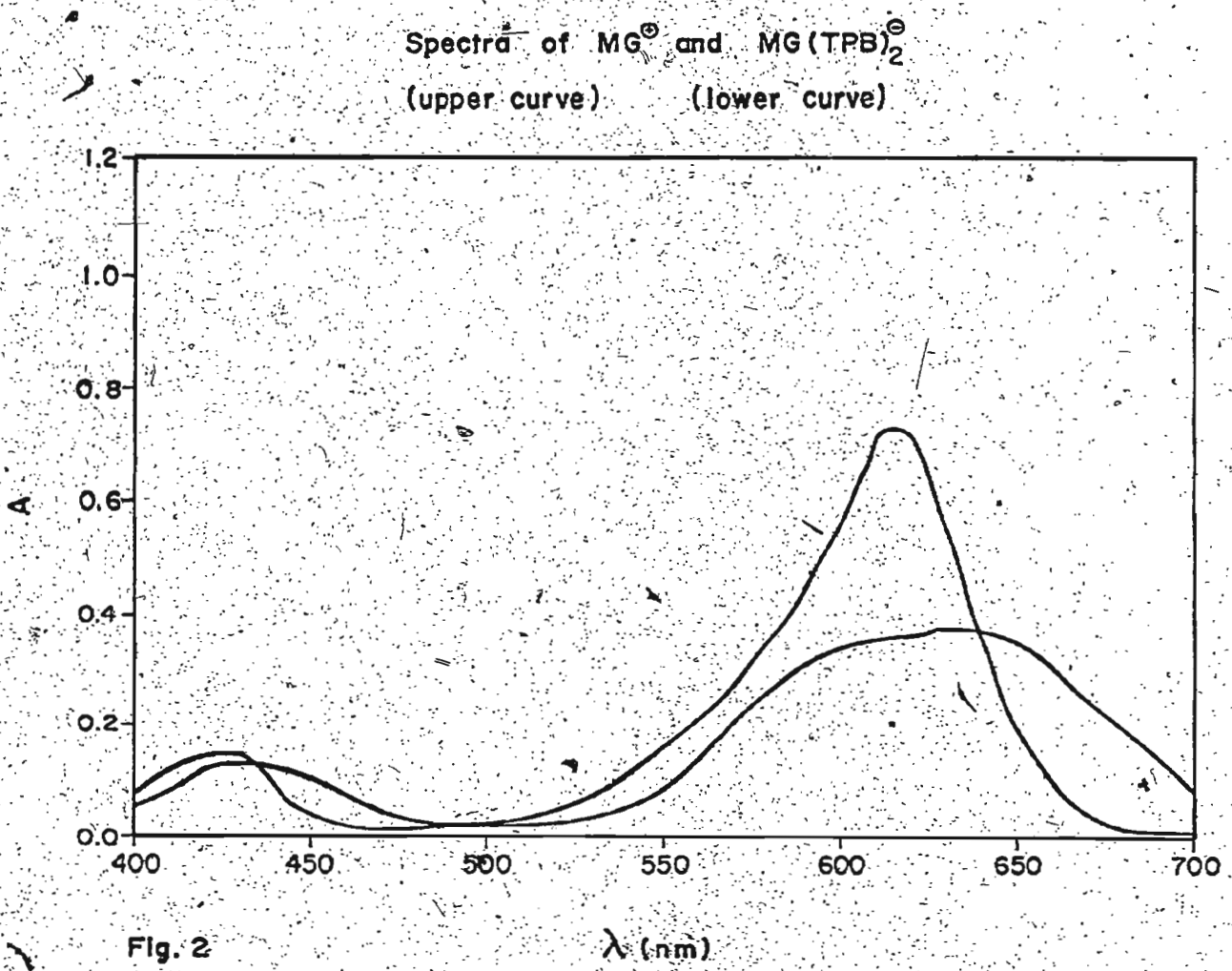
Spectra of $MG^{\oplus}$ and $MG(TPB)_2^{\ominus}$
(upper curve) (lower curve)
1.2
1.0
0.8
0.6
0.4
0.2
0.0
A
400
450
500
550
600
650
700
λ (nm)

Fig. 2

Table 1a

Dependence of absorbance on trityl ion concentration:

$[TPB^{\theta}]$ = 11.345 x 10^{-4}M (fig. 3)

$[pMeOMG^{\bullet}](x\ 10^{-6}M)$*	%T	A
2.346	84.3	0.074
4.692	68.2	0.166
7.038	58.0	0.237
9.384	47.7	0.321
11.73	38.7	0.412
14.08	32.1	0.493
16.42	26.7	0.573
21.11	18.3	0.738
23.46	15.0	0.824

slope = 3.54 ± 0.02 x $10^{4}M^{-1}cm^{-1}$ y-int = -0.0069 ± 0.0028

*The expression in the brackets is the units. e.g. The first entry in this column is 2.346 x 10^{-6}M.

Table 1b

Dependence of absorbance on trityl ion concentration:

$[TPB^{\oplus}] = 2.276 \times 10^{-4} M$ (fig. 3)

$[pMeOMG^{\oplus}]$ ($\times 10^{-6} M$)	%T	A
2.346	82.9	0.081
4.692	67.9	0.168
7.038	56.0	0.252
9.384	48.3	0.316
11.73	38.9	0.410
16.42	27.8	0.556
18.77	24.0	0.620
21.11	17.8	0.750
23.46	15.9	0.799

slope = $3.40 \pm 0.07 \times 10^{4} M^{-1} cm^{-1}$ y-int = 0.0046 ± 0.0102

Combined data from Tables 1a and 1b:

slope = $3.47 \pm 0.04 \times 10^{4} M^{-1} cm^{-1}$ y-int = -0.0008 ± 0.0057

Plot of Absorbance –vs– $[pMeOMGClO_4]$

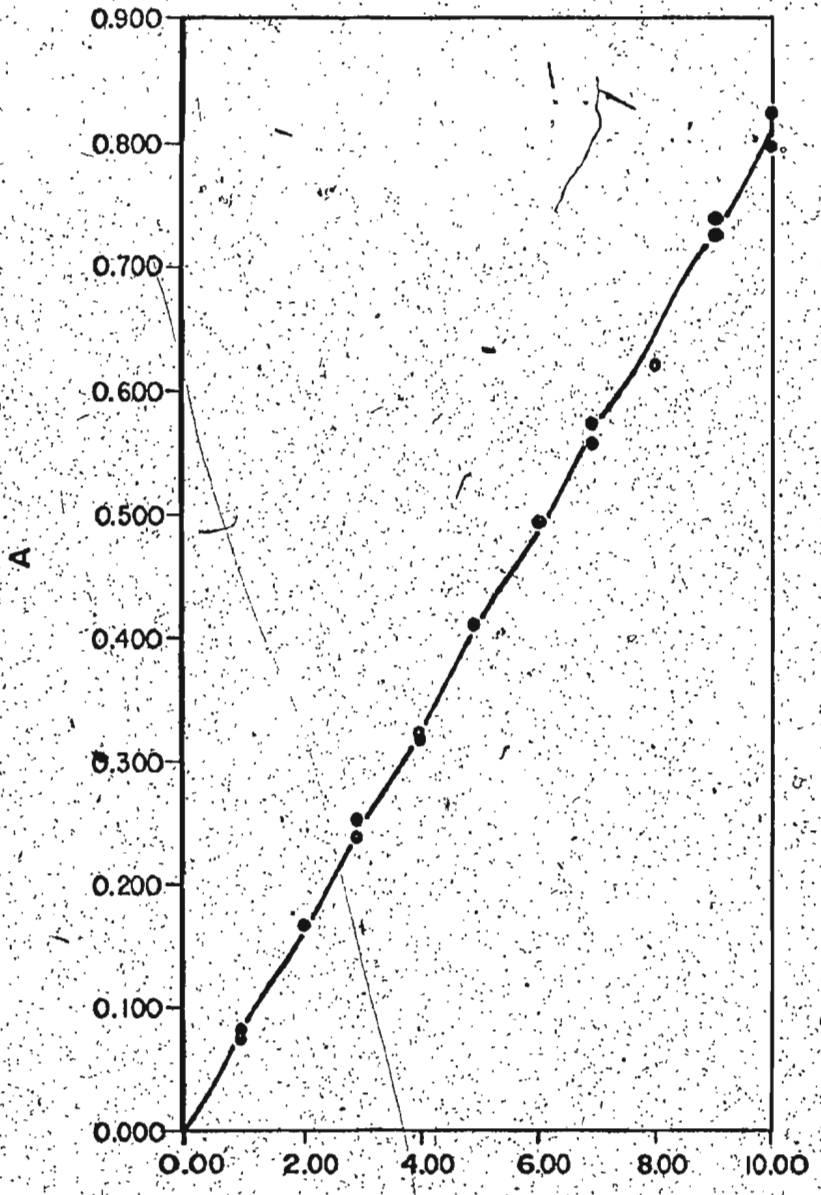

Fig.3 $[pMeOMGClO_4]$ (x 2.346 x 10^{-4} M)

Table 2a

Dependence of absorbance on trityl ion concentration:

$[TPB^{\theta}] = 11.345 \times 10^{-4} M$ (fig. 4)

$[MG^{\oplus}]$ ($\times 10^{-6} M$)	%T	A
2.757	82.2	0.085
5.514	67.9	0.168
8.271	56.8	0.246
11.03	47.3	0.325
13.79	39.3	0.406
16.54	32.0	0.495
19.30	26.2	0.582
22.06	21.9	0.660
24.81	18.7	0.728
27.57	15.3	0.815

slope = $2.95 \pm 0.02 \times 10^{4} M^{-1} cm^{-1}$ y-int = 0.0036 ± 0.0036

Table 2b

Dependence of absorbance on trityl ion concentration:

$[TPB^{\ominus}] = 2.269 \times 10^{-4} M$ (fig. 4)

$[MG^{\oplus}](\times 10^{-6} M)$	XT	A
2.757	84.2	0.075
5.514	67.9	0.168
8.271	56.0	0.252
11.03	45.4	0.343
13.79	37.1	0.431
16.54	30.8	0.511
19.30	26.8	0.572
22.06	20.9	0.680
24.81	18.8	0.726
27.57	14.9	0.827

slope = $2.99 \pm 0.05 \times 10^{4} M^{-1} cm^{-1}$ y-int = 0.0058 ± 0.0088

Combined data from Tables 2a and 2b:

slope = $2.97 \pm 0.03 \times 10^{4} M^{-1} cm^{-1}$ y-int = 0.0047 ± 0.0049

Plot of Absorbance -vs- [MGCl]

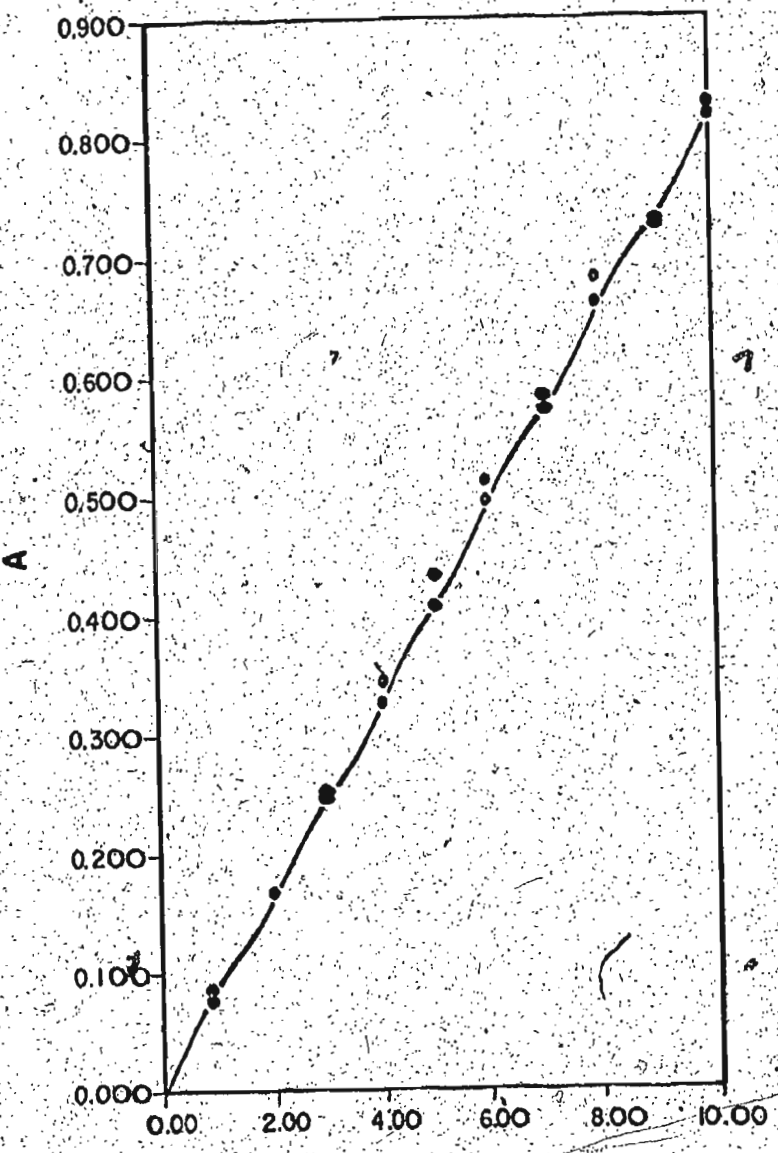

Fig. 4

Table 3

The reactions of $pMeOMGSO_3^{\ominus}$ with $TPB^{\ominus}$:

$[TPB^{\ominus}] = 11.080 \times 10^{-4}$ M (fig. 5)

k_{obs} ($\times 10^{-3} s^{-1}$)	k_{obs}^{-1} (s)	$[SO_3^{2\ominus}]$ ($\times 10^{-3}$ M)
7.136 ± 0.024	140.1	0.95
4.914 ± 0.026	203.5	2.22
4.900 ± 0.020	204.1	2.94
4.720 ± 0.029	211.9	4.01
3.593 ± 0.013	278.3	5.03
3.242 ± 0.017	308.5	6.15
3.055 ± 0.026	327.3	6.91
2.503 ± 0.018	399.5	9.00

Reaction of $pMeOMGSO_3^{\ominus}$ with $TPB^{\ominus}$

$[TPB^{\ominus}] = 11.080 \times 10^{-4}\,M$

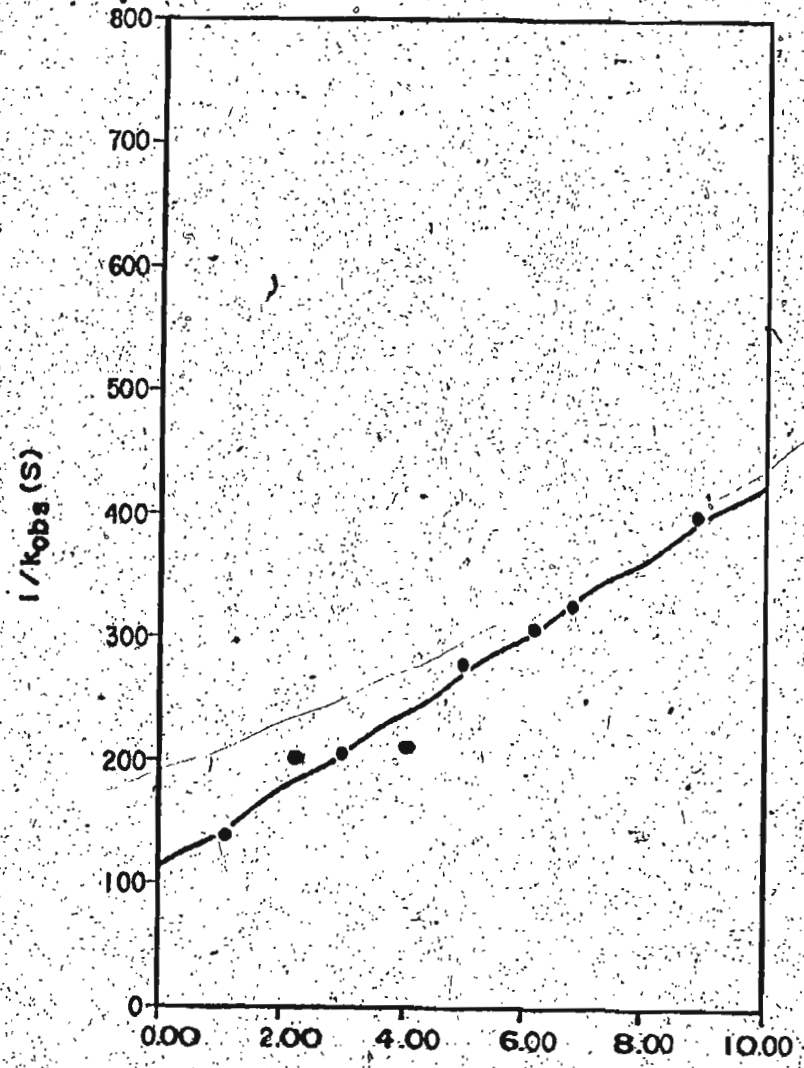

Fig. 5

Table 4

The reactions of $pMeOMGSO_3^{\ominus}$ with $TPB^{\ominus}$:

$[TPB^{\ominus}] = 8.864 \times 10^{-4}M$ (fig. 6)

k_{obs} ($\times 10^{-3} s^{-1}$)	k_{obs}^{-1} (s)	$[SO_3^{2\ominus}]$ ($\times 10^{-3}M$)
7.127 ± 0.033	140.3	1.09
6.125 ± 0.026	163.3	1.94
4.851 ± 0.020	206.1	2.99
4.535 ± 0.038	220.5	4.35
3.960 ± 0.018	252.5	5.26
3.701 ± 0.016	270.2	6.24
3.080 ± 0.031	324.7	7.14
2.600 ± 0.014	384.6	7.98

Reaction of $pMeOMGSO_3^{\ominus}$ with $TPB^{\ominus}$

$[TPB^{\ominus}] = 8.864 \times 10^{-4} M$

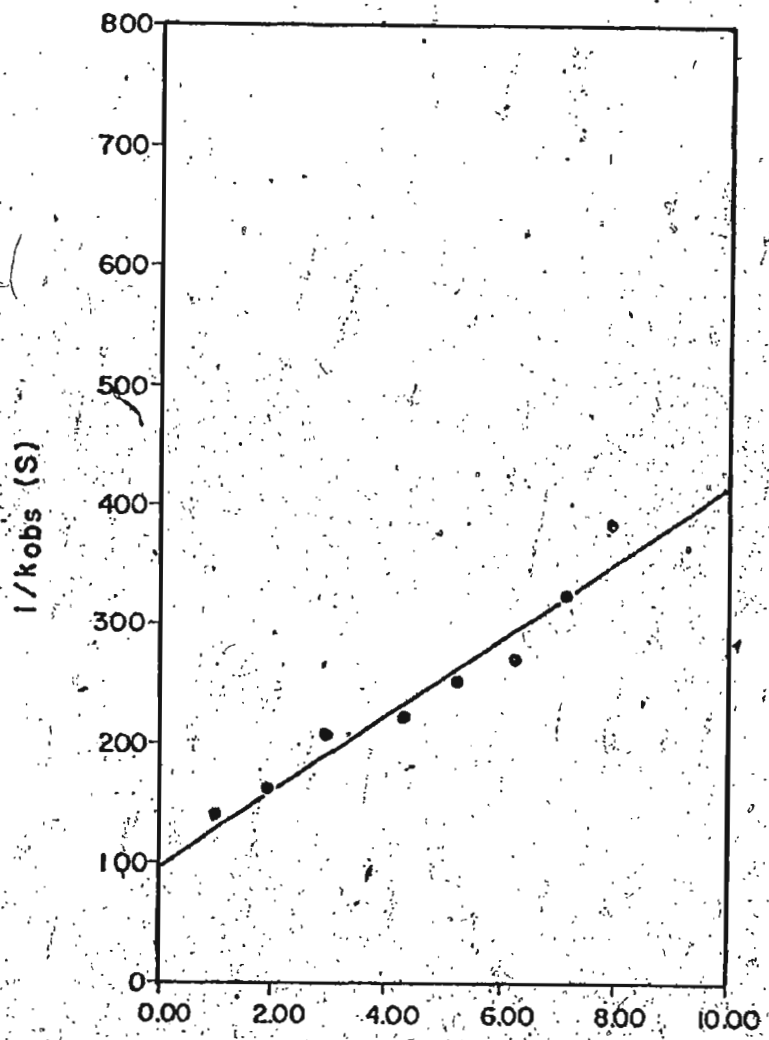

Fig. 6

Table 5

The reactions of $pMeOMGSO_3^{\theta}$ with TPB^{θ}:

$[TPB^{\theta}] = 6.650 \times 10^{-4}M$ (fig. 7)

$k_{obs}(\times 10^{-3}s^{-1})$	$k_{obs}^{-1}(s)$	$[SO_3^{2\theta}](\times 10^{-3}M)$
6.374 ± 0.022	156.9	1.00
4.366 ± 0.016	229.0	2.14
3.665 ± 0.022	272.9	3.15
3.629 ± 0.015	275.6	4.27
2.915 ± 0.018	343.1	4.92
2.471 ± 0.010	404.7	6.03
2.339 ± 0.018	427.5	6.80

Reaction of $pMeOMGSO_3^{\ominus}$ with $TPB^{\ominus}$

$[TPB^{\ominus}] = 6.650 \times 10^{-4}$ M

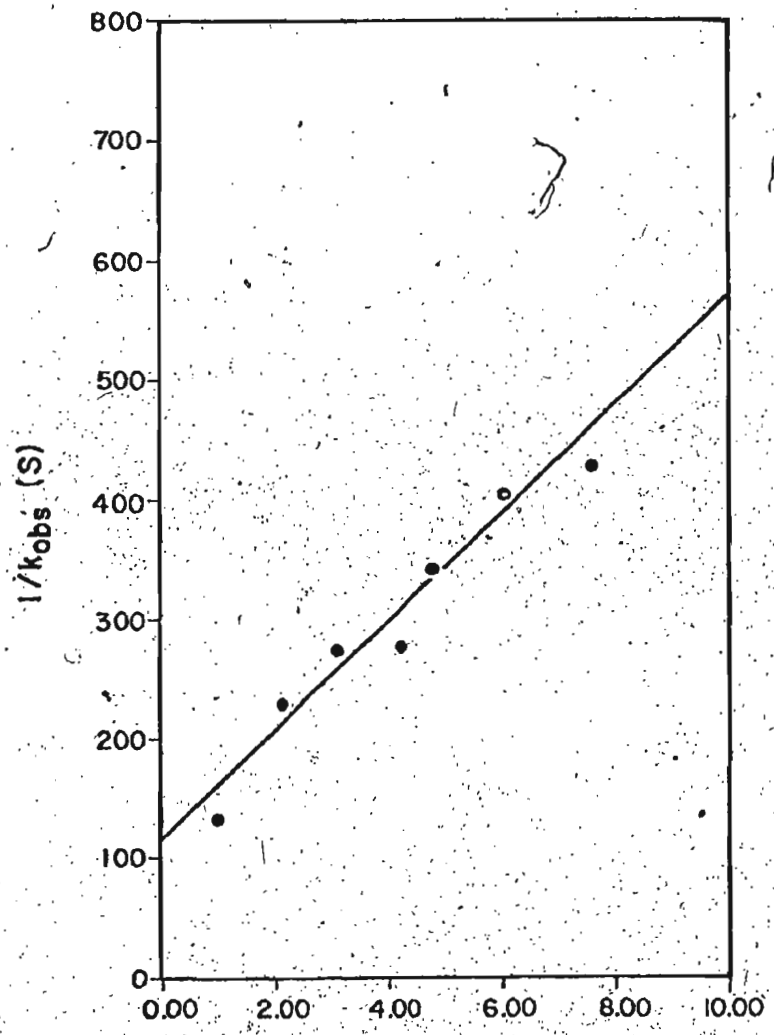

Fig. 7

Table 6

The reactions of $pMeOMGSO_3^{\theta}$ with TPB^{θ}:

$[TPB^{\theta}] = 5.320 \times 10^{-4}$ M (fig. 8)

k_{obs} ($\times 10^{-3}$ s^{-1})	k_{obs}^{-1} (s)	$[SO_3^{2\theta}]$ ($\times 10^{-3}$ M)
5.696 ± 0.014	175.6	1.22
4.222 ± 0.025	236.9	2.09
4.134 ± 0.018	241.9	2.87
3.654 ± 0.016	273.7	3.94
2.778 ± 0.013	360.0	4.98
2.005 ± 0.013	498.8	8.09
1.602 ± 0.010	624.2	9.28

Reaction of $pMeOMGSO_3^{\ominus}$ with $TPB^{\ominus}$

$[TPB^{\ominus}] = 5.320 \times 10^{-4} M$

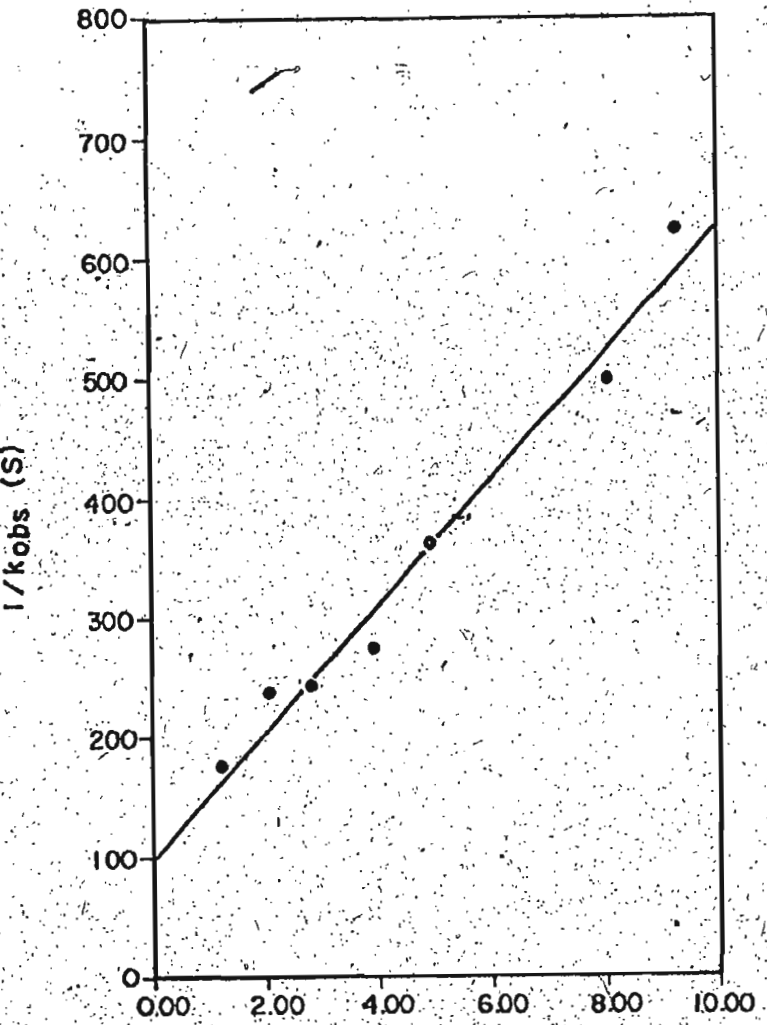

Fig. 8

Table 7

The reactions of $pMeOMGSO_3^{\ominus}$ with $TPB^{\ominus}$:

$[TPB^{\ominus}] = 4.433 \times 10^{-4}$ M (fig. 9)

k_{obs} ($\times 10^{-3} s^{-1}$)	k_{obs}^{-1} (s)	$[SO_3^{2\ominus}]$ ($\times 10^{-3}$ M)
5.916 ± 0.036	169.0	1.02
4.824 ± 0.015	207.3	1.93
3.507 ± 0.015	285.1	2.88
2.889 ± 0.016	346.1	4.24
2.667 ± 0.017	375.0	5.03
2.554 ± 0.017	391.5	6.04
2.219 ± 0.012	450.7	6.87
1.689 ± 0.011	592.1	10.23

Reaction of $pMeOMGSO_3^{\ominus}$ with $TPB^{\ominus}$

$[TPB^{\ominus}] = 4.433 \times 10^{-4}$ M

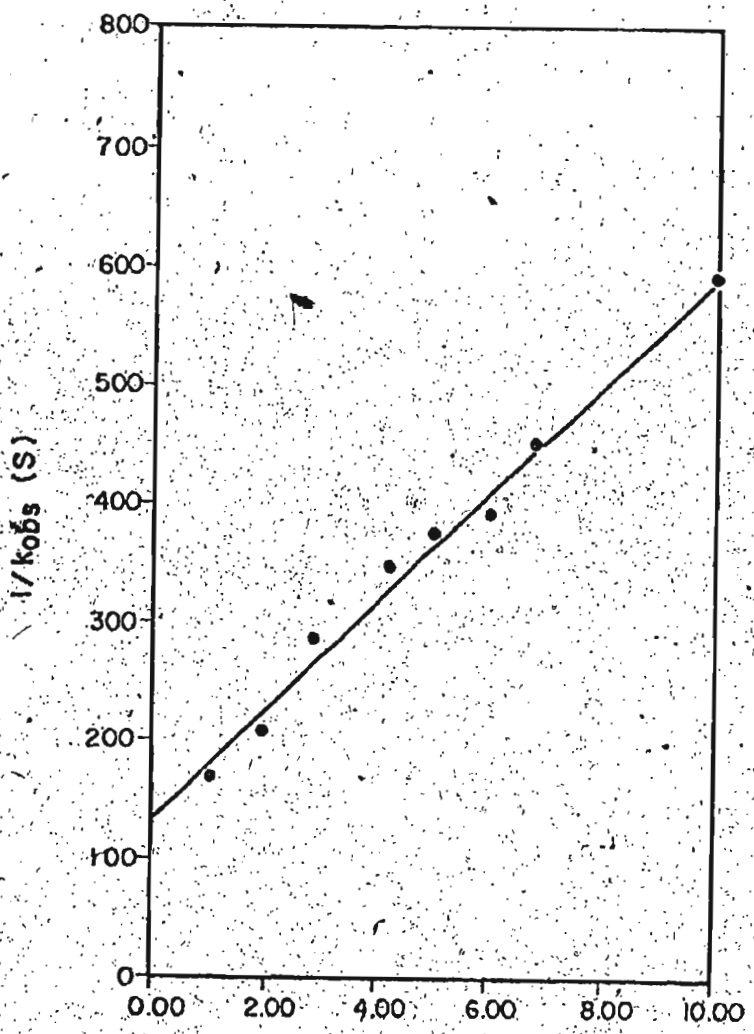

Fig. 9

Table 8

The reactions of $pMeOMGSO_3^{\ominus}$ with $TPB^{\ominus}$:

$[TPB^{\ominus}] = 3.546 \times 10^{-4}$ M (fig. 10)

k_{obs} ($\times 10^{-3}$ s^{-1})	k_{obs}^{-1} (s)	$[SO_3^{2\ominus}]$ ($\times 10^{-3}$ M)
8.532 ± 0.134	117.2	1.04
4.819 ± 0.024	207.5	2.19
4.800 ± 0.023	208.3	2.99
3.402 ± 0.014	293.9	3.93
2.100 ± 0.014	476.2	5.22
2.328 ± 0.012	429.6	6.09
1,953 ± 0.013	512.0	6.86
1.736 ± 0.011	576.0	8.13

Reaction of $pMeOMGSO_3^{\ominus}$ with $TPB^{\ominus}$

$[TPB^{\ominus}] = 3.546 \times 10^{-4} M$

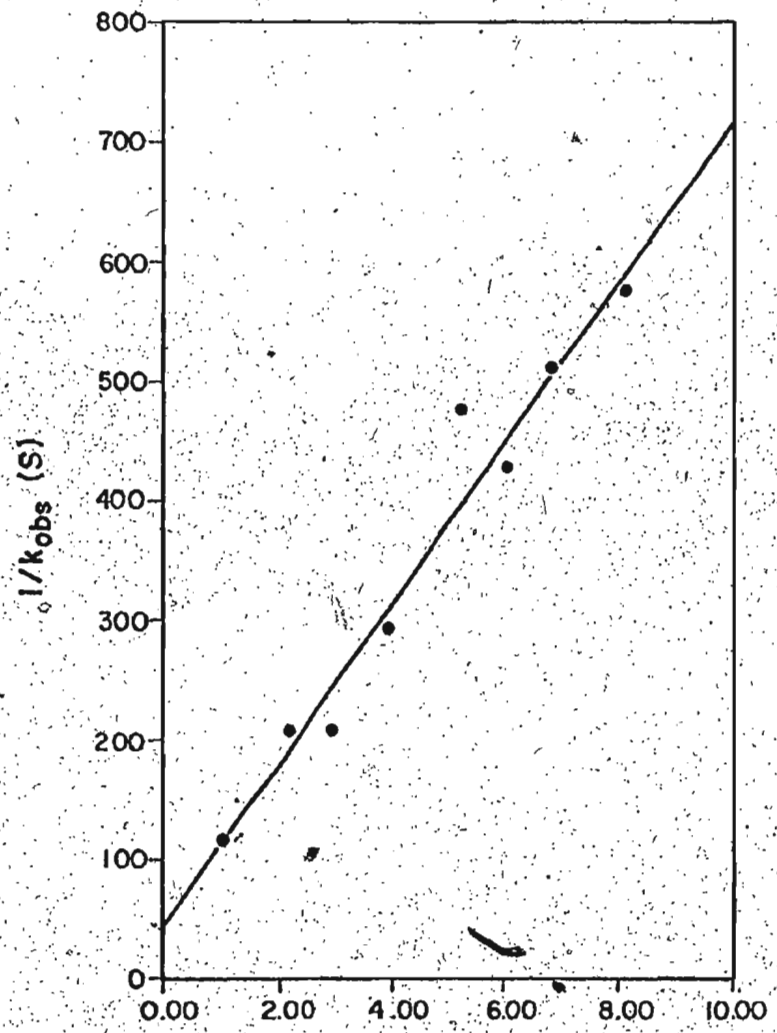

Fig. 10

Table 9

The reactions of $pMeOMGSO_3^{\ominus}$ with $TPB^{\ominus}$:

$[TPB^{\ominus}] = 2.660 \times 10^{-4}$ M (fig. 11)

k_{obs} ($\times 10^{-3} s^{-1}$)	k_{obs}^{-1} (s)	$[SO_3^{2\ominus}]$ ($\times 10^{-3}$ M)
6.289 ± 0.019	159.0	1.10
3.696 ± 0.008	270.6	2.17
3.383 ± 0.015	295.6	3.10
1.767 ± 0.009	565.9	6.02
1.547 ± 0.009	646.4	7.05

Reaction of $pMeOMGSO_3^{\ominus}$ with $TPB^{\ominus}$

$[TPB^{\ominus}] = 2.660 \times 10^{-4}$ M

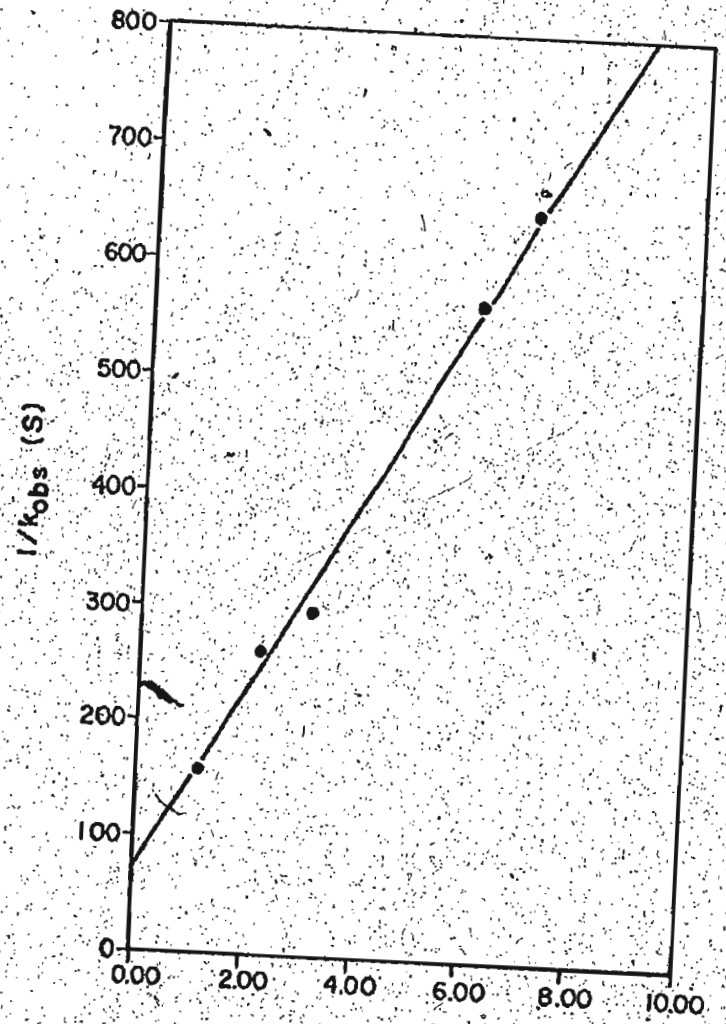

Fig. II

Table 10

The reactions of $pMeOMGSO_3^{\ominus}$ with $TPB^{\ominus}$:

$[TPB^{\ominus}] = 2.217 \times 10^{-4}$ M (fig. 12)

k_{obs} ($\times 10^{-3} s^{-1}$)	k_{obs}^{-1} (s)	$[SO_3^{2\ominus}]$ ($\times 10^{-3}$ M)
4.626 ± 0.026	216.2	1.10
4.204 ± 0.024	237.9	2.00
2.695 ± 0.009	371.1	2.92
1.692 ± 0.008	591.0	6.31
1.398 ± 0.010	715.3	8.02

Reaction of $pMeOMGSO_3^{\ominus}$ with $TPB^{\ominus}$

$[TPB^{\ominus}] = 2.217 \times 10^{-4}$ M

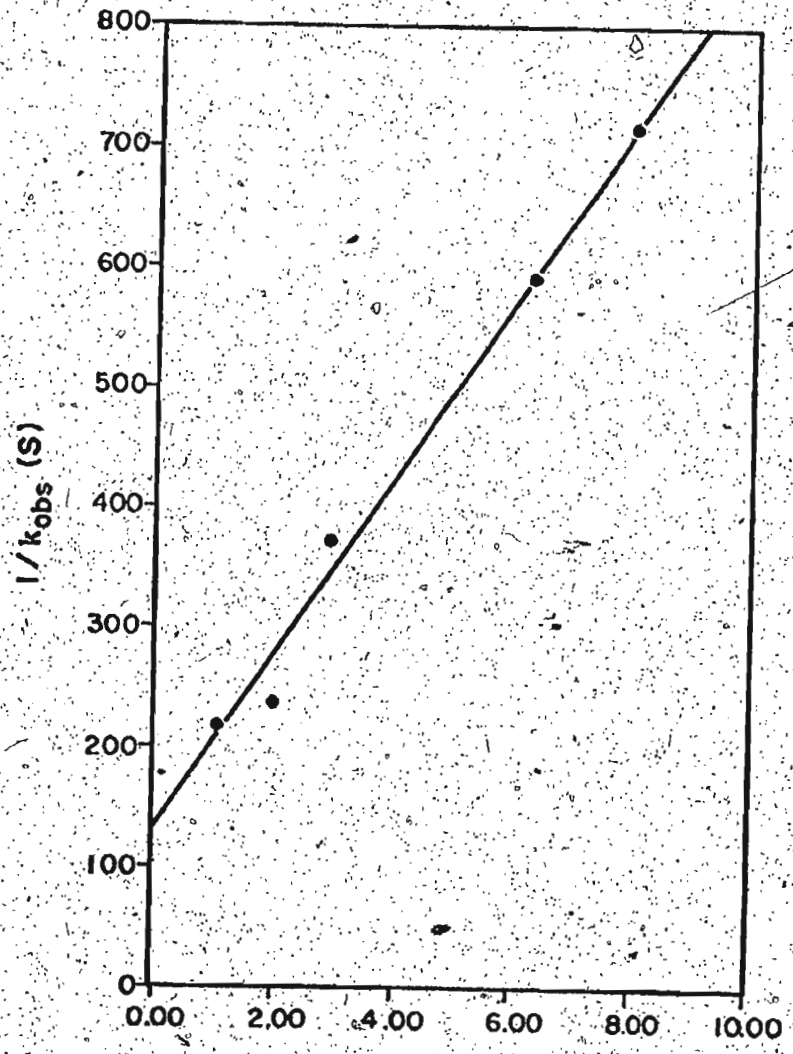

Fig. 12

Table 11

The reactions of $MGSO_3^{\theta}$ with TPB^{θ}:

$[TPB^{\theta}] = 11.335 \times 10^{-4} M$ (fig. 13)

k_{obs} ($\times 10^{-4} s^{-1}$)	k_{obs}^{-1} (s)	$[SO_3^{2\theta}]$ ($\times 10^{-4} M$)
21.45 ± 0.05	466	4.7
16.27 ± 0.05	615	9.9
13.14 ± 0.06	761	14.8
11.56 ± 0.03	865	19.4
10.25 ± 0.04	976	26.8
8.697 ± 0.045	1150	31.5
8.061 ± 0.033	1241	40.5
6.701 ± 0.023	1492	46.3

Reaction of $MGSO_3^{\ominus}$ with $TPB^{\ominus}$

$[TPB^{\ominus}] = 11.335 \times 10^{-4}\ M$

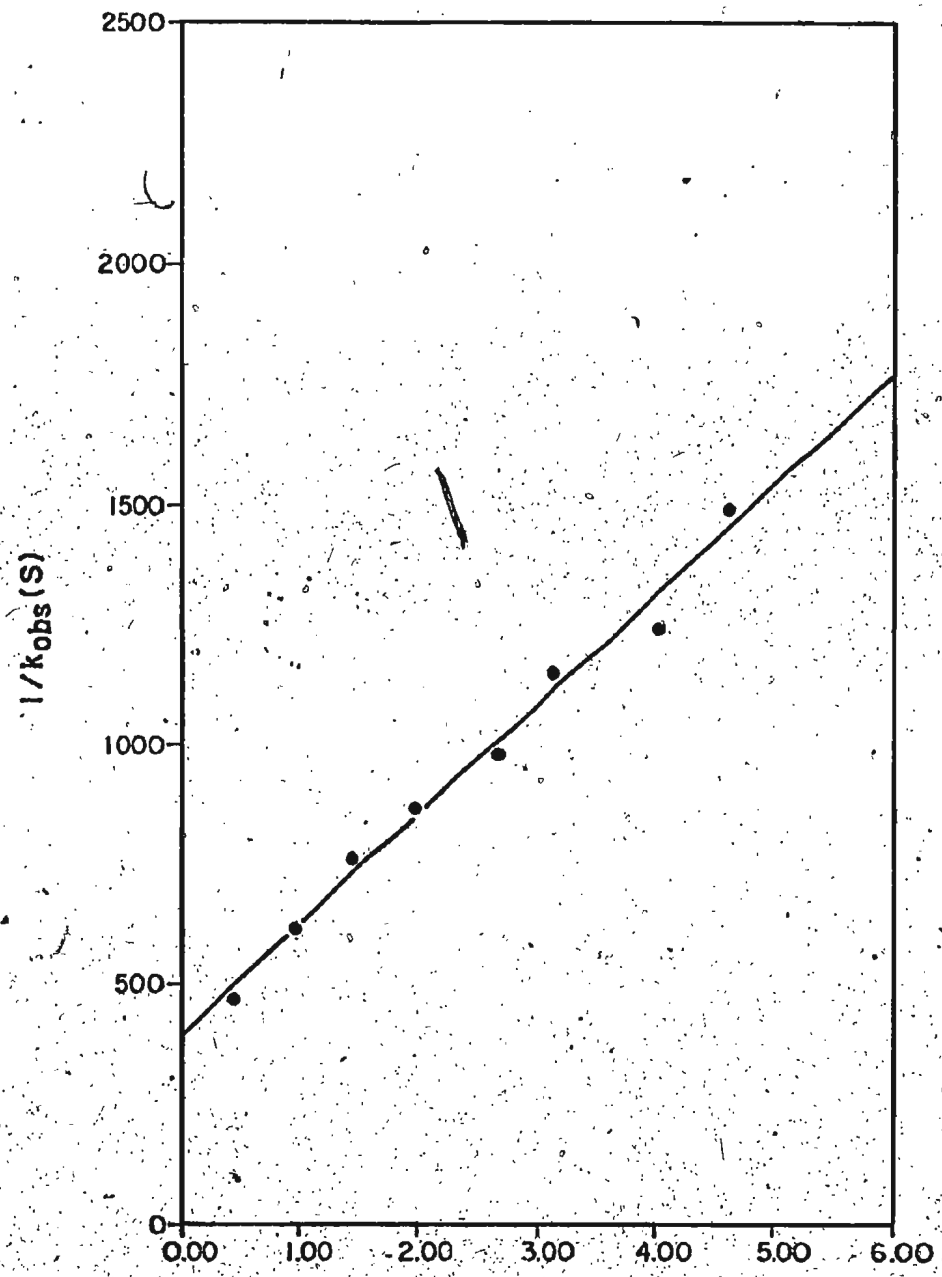

Fig. 13

Table 12

The reactions of $MGSO_3^{\theta}$ with TPB^{θ}:

$[TPB^{\theta}] = 9.068 \times 10^{-4} M$ (fig. 14)

k_{obs} ($\times 10^{-4} s^{-1}$)	k_{obs}^{-1} (s)	$[SO_3^{2\theta}]$ ($\times 10^{-4} M$)
20.67 ± 0.05	484	5.3
17.40 ± 0.05	575	10.2
14.36 ± 0.04	695	16.0
11.50 ± 0.03	870	21.6
10.89 ± 0.04	918	24.8
8.466 ± 0.033	1181	30.5
8.405 ± 0.031	1190	33.6

Reaction of $MGSO_3^{\ominus}$ with $TPB^{\ominus}$

$[TPB^{\ominus}] = 9.068 \times 10^{-4}\,M$

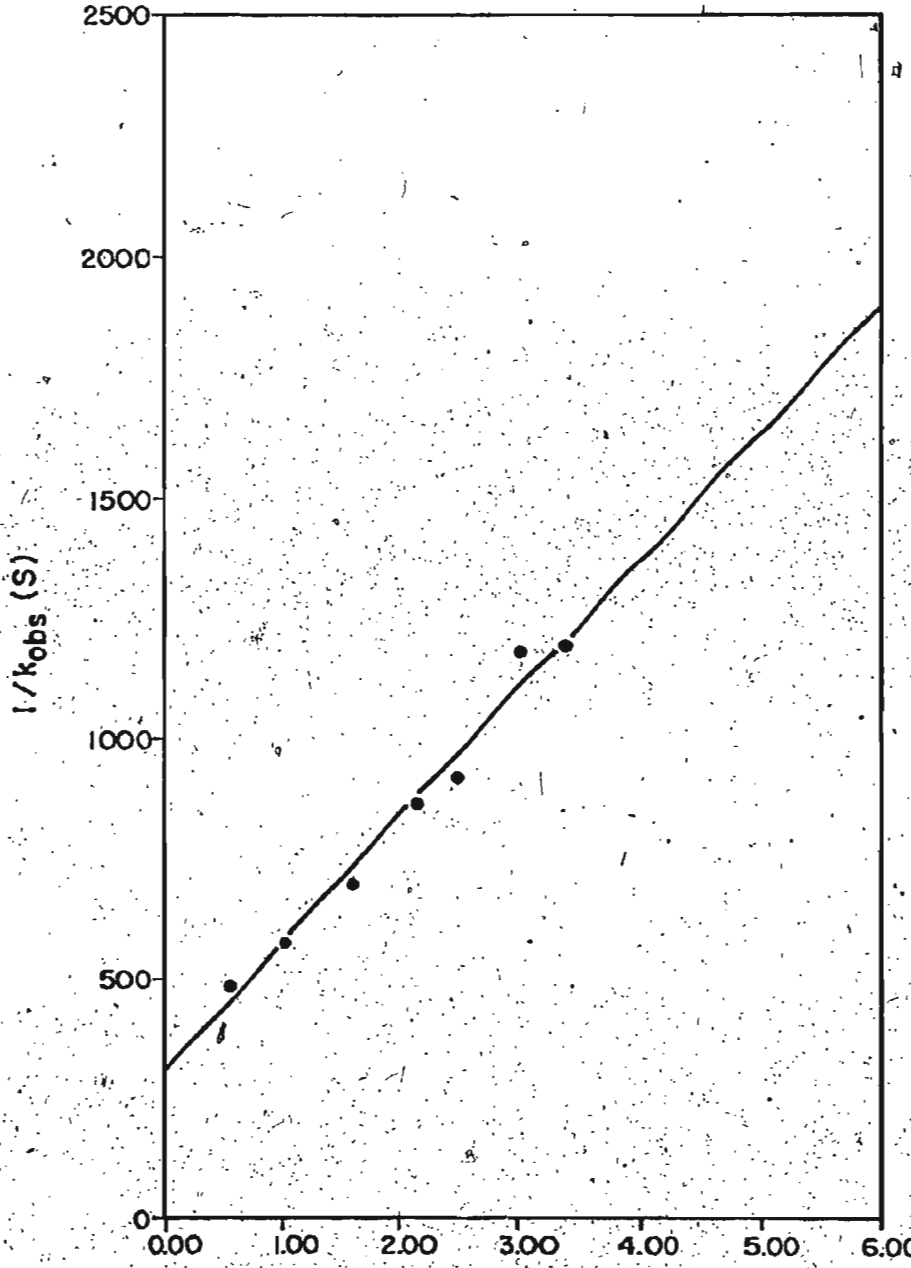

Fig. 14

Table 13

The reactions of $MGSO_3^{\theta}$ with TPB^{θ}:

$[TPB^{\theta}] = 6.801 \times 10^{-4}$ M (fig. 15)

k_{obs} ($\times 10^{-4} s^{-1}$)	k_{obs}^{-1} (s)	$[SO_3^{2\theta}]$ ($\times 10^{-4}$ M)
18.33 ± 0.06	546	6.9
16.21 ± 0.04	617	9.5
14.30 ± 0.05	699	15.7
9.748 ± 0.030	1026	20.6
10.34 ± 0.04	967	25.4
8.042 ± 0.031	1243	29.1
8.496 ± 0.073	1177	33.9
5.504 ± 0.028	1817	45.9

Reaction of $MGSO_3^{\ominus}$ with $TPB^{\ominus}$

$[TPB^{\ominus}] = 6.801 \times 10^{-4} M$

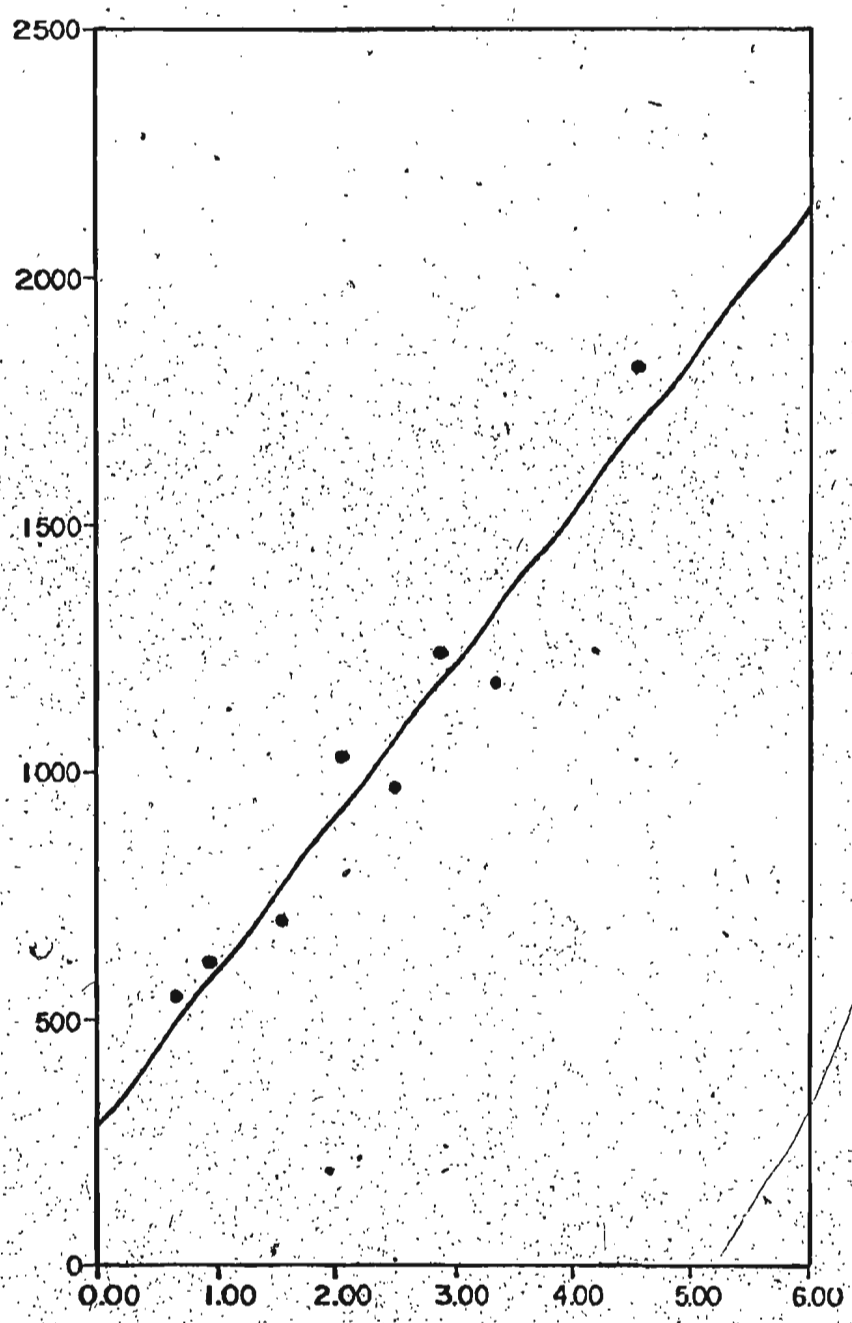

Fig. 15

Table 14

The reactions of $MGSO_3^{\theta}$ with TPB^{θ}:

$[TPB^{\theta}] = 5.441 \times 10^{-4}$ M (fig. 16)

k_{obs} ($\times 10^{-4} s^{-1}$)	k_{obs}^{-1} (s)	$[SO_3^{2\theta}]$ ($\times 10^{-4}$ M)
19.25 ± 0.07	519	5.7
13.84 ± 0.05	723	10.1
12.56 ± 0.05	796	15.6
9.012 ± 0.031	1110	20.5
8.785 ± 0.076	1138	25.1
6.386 ± 0.047	1566	29.9
6.166 ± 0.040	1622	37.3
5.861 ± 0.049	1706	42.2
4.634 ± 0.025	2158	49.3

Reaction of $MGSO_3^{\ominus}$ with $TPB^{\ominus}$

$[TPB^{\ominus}] = 5.441 \times 10^{-4}$ M

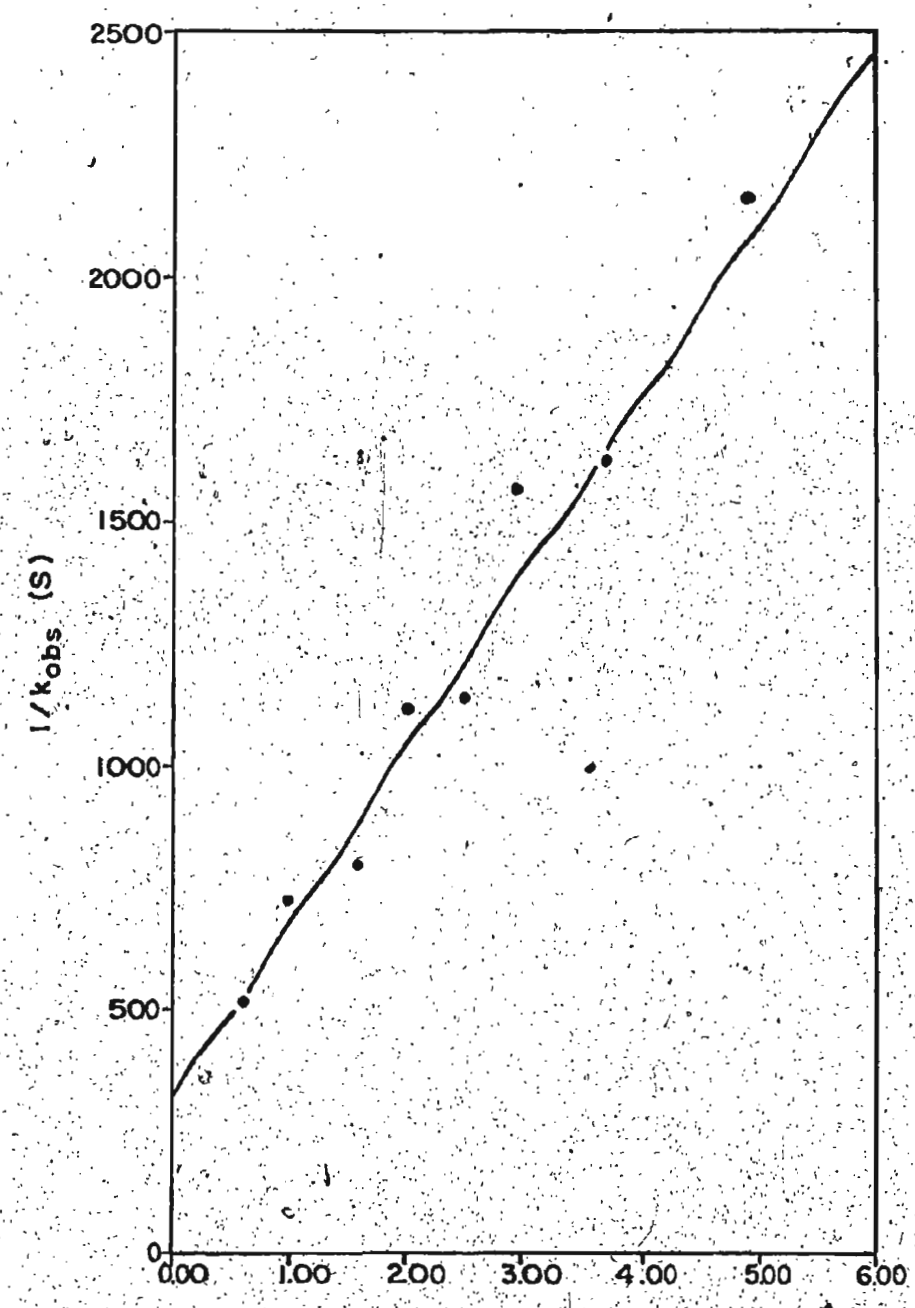

Fig. 16

Table 15

The reactions of $MGSO_3^{\theta}$ with TPB^{θ}:

$[TPB^{\theta}] = 4.543 \times 10^{-4} M$ (fig. 17)

k_{obs} ($\times 10^{-4} s^{-1}$)	k_{obs}^{-1} (s)	$[SO_3^{2\theta}]$ ($\times 10^{-4} M$)
20.88 ± 0.09	479	4.9
13.77 ± 0.05	726	10.1
12.17 ± 0.09	822	15.9
7.183 ± 0.042	1392	25.5
5.357 ± 0.035	1867	35.4
4,581 ± 0.032	2183	45.3
4.340 ± 0.028	2304	49.3

Reaction of $MGSO_3^{\ominus}$ with $TPB^{\ominus}$

$[TPB^{\ominus}] = 4.543 \times 10^{-4}$ M

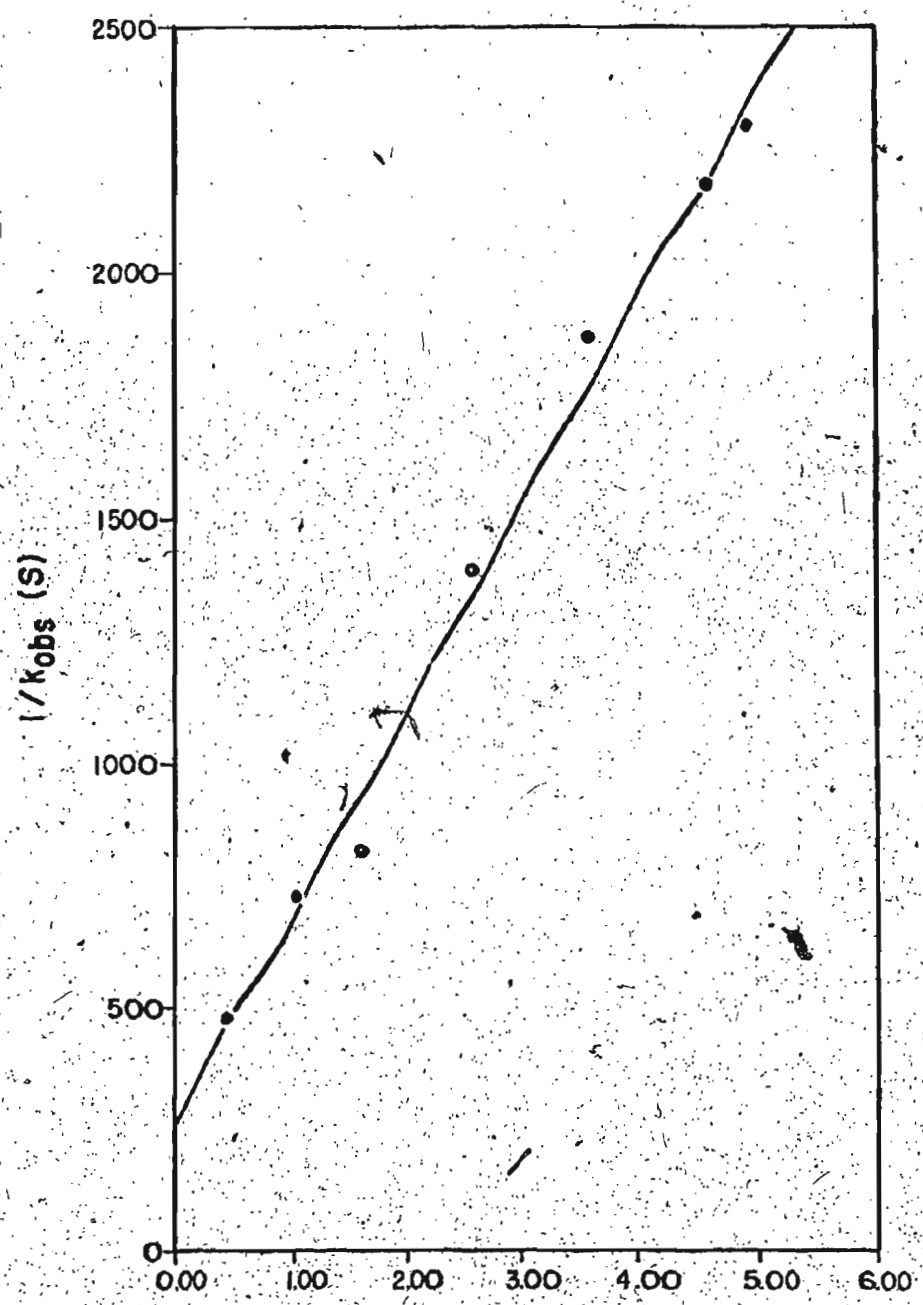

Fig. 17

Table 16

The reactions of $MGSO_3^{\theta}$ with TPB^{θ}:

$[TPB^{\theta}] = 3.634 \times 10^{-4} M$ (fig. 18)

k_{obs} ($\times 10^{-4} s^{-1}$)	k_{obs}^{-1} (s)	$[SO_3^{2\theta}]$ ($\times 10^{-4} M$)
19.84 ± 0.05	504	6.1
17.42 ± 0.11	574	9.8
10.82 ± 0.07	924	15.0
10.19 ± 0.05	981	19.8
8.895 ± 0.070	1124	24.9
6.506 ± 0.032	1537	30.2
5.379 ± 0.017	1859	41.0

Reaction of $MGSO_3^{\ominus}$ with $TPB^{\ominus}$

$[TPB^{\ominus}] = 3.634 \times 10^{-4} M$

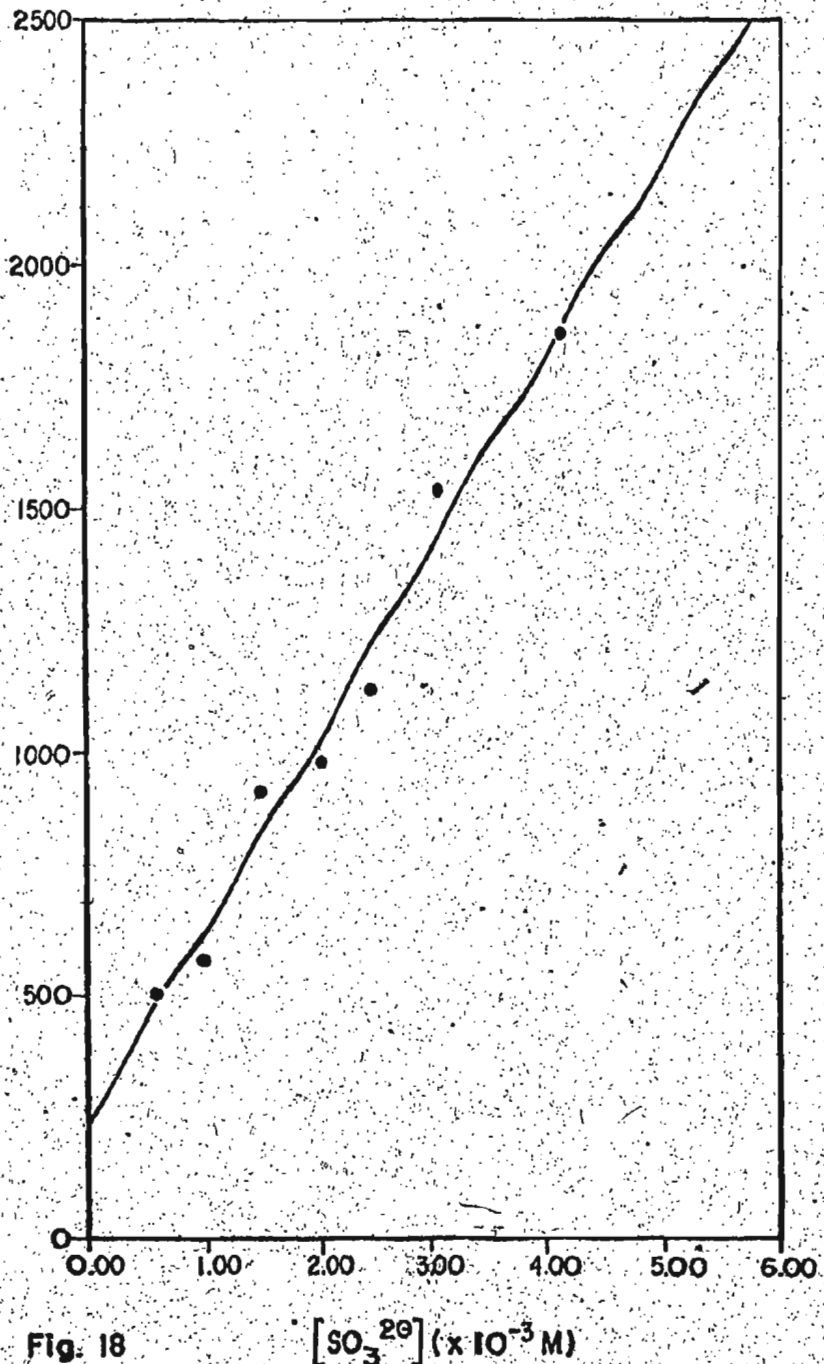

Fig. 18

Table 17

The reactions of $MGSO_3^{\theta}$ with TPB^{θ}:

$[TPB^{\theta}] = 2.726 \times 10^{-4}$ M (fig. 19)

k_{obs} ($\times 10^{-4}$ s^{-1})	k_{obs}^{-1} (s)	$[SO_3^{2\theta}]$ ($\times 10^{-4}$ M)
20.57 ± 0.11	486	5.6
13.30 ± 0.06	752	9.4
11.79 ± 0.13	848	15.2
8.138 ± 0.050	1229	20.3
6.174 ± 0.035	1620	30.4
5.676 ± 0.037	1762	35.5
4.874 ± 0.032	2052	44.7

Reaction of $MGSO_3^{\ominus}$ with $TPB^{\odot}$

$[TPB^{\ominus}] = 2.726 \times 10^{-4} M$

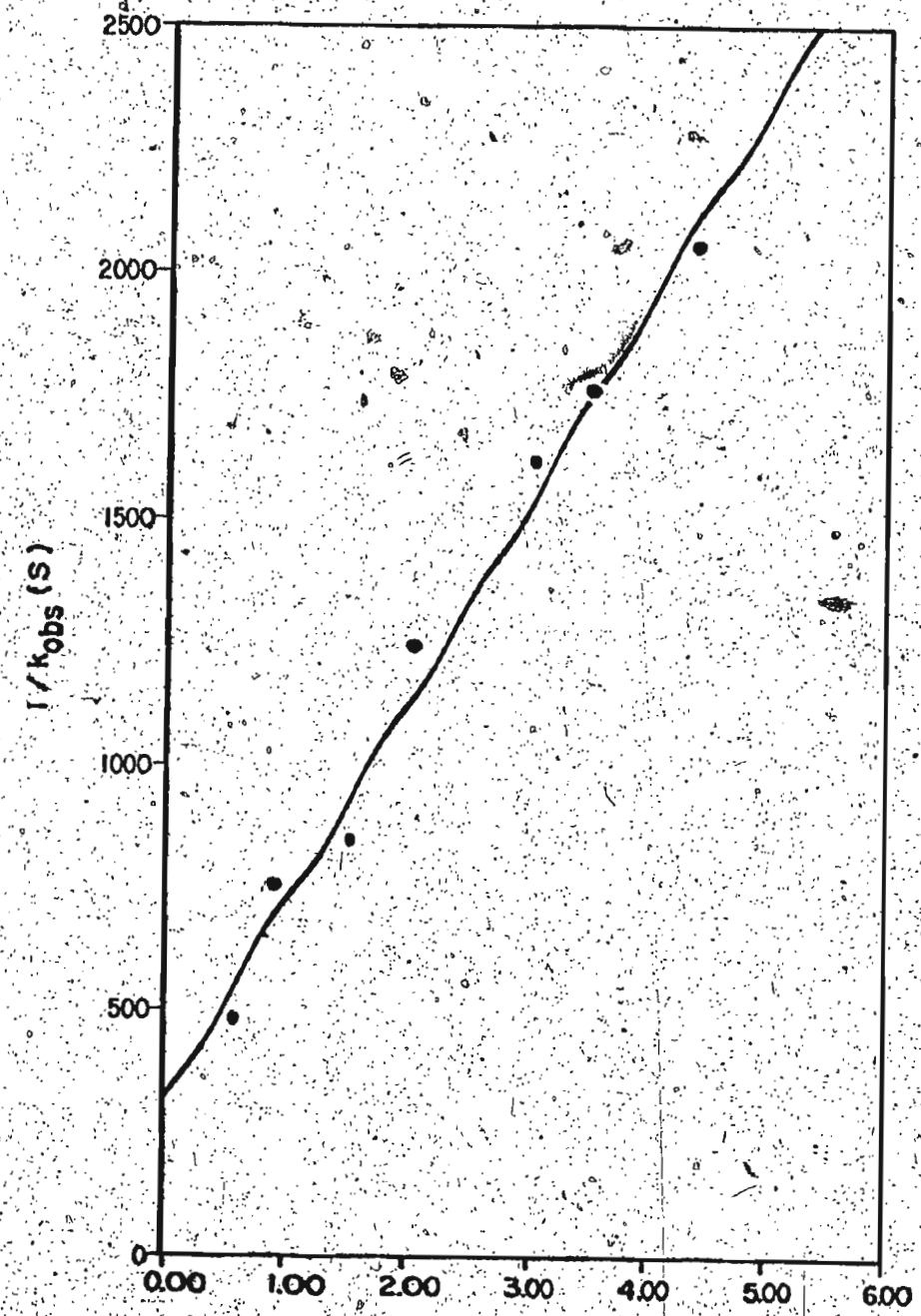

Fig. 19

Table 18

The reactions of $MGSO_3^{\theta}$ with TPB^{θ}:

$[TPB^{\theta}] = 2.272 \times 10^{-4}$ M (fig. 20)

k_{obs} ($\times 10^{-4}$ s^{-1})	k_{obs}^{-1} (s)	$[SO_3^{2\theta}]$ ($\times 10^{-4}$ M)
19.70 ± 0.13	508	6.0
13.99 ± 0.07	715	10.4
10.33 ± 0.06	968	14.9
9.974 ± 0.061	1003	20.1
6.143 ± 0.041	1628	30.2
4.172 ± 0.027	2397	44.9

Reaction of $MGSO_3^{\ominus}$ with $TPB^{\ominus}$

$[TPB^{\ominus}] = 2.272 \times 10^{-4} M$

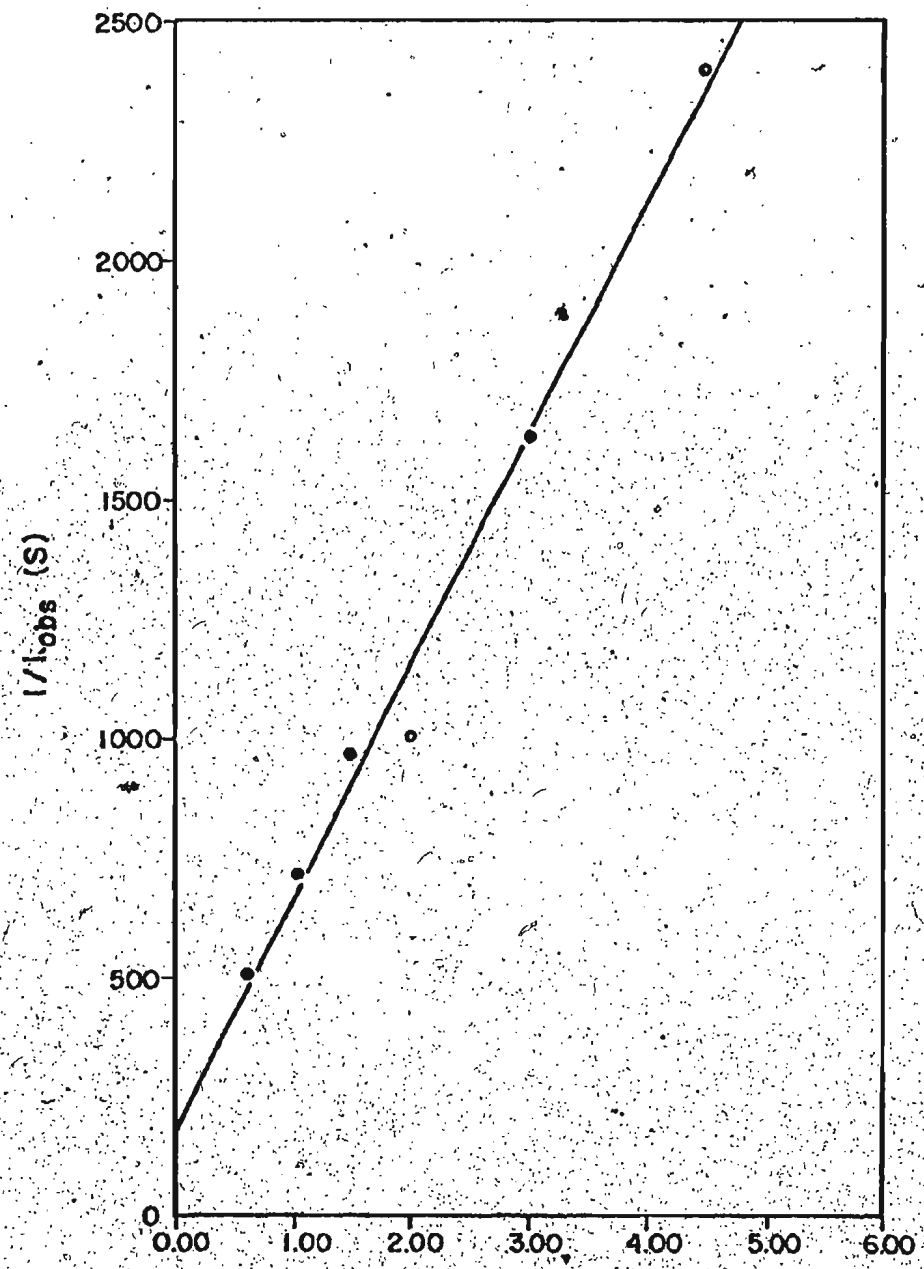

Fig. 20

Table 19

Linear least squares results (Tables 3 to 10):

$pMeOMGSO_3^{\theta}$

$[TPB^{\theta}]$ ($\times 10^{-4}$ M)	slope ($\times 10^{4} M^{-1} s$)	int(s)
11.080	3.132 ± 0.206	113 ± 11
8.864	3.192 ± 0.306	98 ± 16
6.650	4.555 ± 0.378	117 ± 17
5.320	5.271 ± 0.384	100 ± 21
4.433	4.526 ± 0.209	136 ± 12
3.546	6.717 ± 0.607	47 ± 31
2.660	8.147 ± 0.413	71 ± 19
2.217	7.384 ± 0.461	126 ± 22

Table 20

Linear least squares results (Tables 11 to 18):

$MGSO_3^{\theta}$

$[TPB^{\theta}](x\cdot10^{-4}M)$	slope($x\ 10^5 M^{-1}s$)	int(s)
11.335	2.298 ± 0.118	389 ± 33
9.068	2.650 ± 0.169	307 ± 38
6.801	3.089 ± 0.314	289 ± 83
5.441	3.584 ± 0.241	321 ± 72
4.543	4.252 ± 0.181	264 ± 56
3.634	3.984 ± 0.279	237 ± 66
2.726	4.027 ± 0.227	323 ± 60
2.272	4.819 ± 0.273	187 ± 68

Discussion

Preliminary Study

The present study is primarily concerned with the dissociation reaction of sulphite ion from two trityl ions, namely pMeOMG$^{\oplus}$ and MG$^{\oplus}$, using TPB$^{\ominus}$ as a trap for the intermediate carbonium ions produced. The conclusions reported depend partly on some preliminary work in which an attempt was made to study the direct reactions of the trityl ions with TPB$^{\ominus}$. This study was carried out in co-operation with Mr. Fred Steele using stopped flow technique. The reactions between the trityl ions and TPB$^{\ominus}$ were both very fast and complex. We were not able to produce satisfactory second order or third order plots for the variation of the pseudo-first order rate constant as the concentration of TPB$^{\ominus}$ was varied. The difficulty encountered is probably a consequence of two factors: (a) kinetic complexity and (b) the absorbances of the solutions at any time are related to the concentrations of several species since the substrate, any of a variety of intermediates (which may include desolvated trityl ion and varying degrees and stoichiometries of ionic association between the trityl ion and TPB$^{\ominus}$) and the product are all possibly absorbing species. This strongly contrasts with the situation when nucleophiles forming a covalent bond are used since the products then no longer absorb in the visible region. However, two important conclusions arise from this work; the first is that the direct reaction of

TPB^{θ} on the trityl ions is faster than any nucleophile yet studied ('k_2' ca. $1 \times 10^4 M^{-1}s^{-1}$) and the second is there is a component of the rate which is probably second order with respect to TPB^{θ}, (i.e. The best kinetic description of the rate law that we found, although inadequate, includes the formation of ion-triplet, $R^{\theta}(TPB^{\theta})_2$.) This suggests that the final product when the concentration of TPB^{θ} is much greater than the concentration of trityl ion is the ion-triplet and this assumption underpins all of the subsequent discussion.

Beer's Law Determination

The spectra of the trityl salts and the complexed trityl ions in the presence of TPB^{θ} are shown in Figures 1 and 2. The concentrations of $pMeOMG^{\theta}$ and MG^{θ} were respectively 1.408×10^{-5} M and 1.667×10^{-5} M. For the TPB^{θ} complexed ions, the trityl ion concentrations were, the same as given above and the TPB^{θ} concentrations were 1.135×10^{-3} M. The spectra indicate the formation of a new species since the original bands are broadened and the intensity of the bands are changed.

Figures 3 and 4 (data in Tables 1 and 2) show the dependence of the absorbance of the product as a function of the trityl ion concentration. A series of trityl ion concentrations were examined at two TPB^{θ} concentrations. The final absorbances were independent of the TPB^{θ} concentration for both trityl ions, giving extinction coefficients of 3.47

$\pm$ 0.04 x $10^4 M^{-1}cm^{-1}$ and 2.97 $\pm$ 0.03 x $10^4 M^{-1}cm^{-1}$ for $pMeOMG^{\oplus}$ and $MG^{\oplus}$ respectively. The linearity of these two plots indicates two things: (a) Since the plots are the same, at two widely different $TPB^{\ominus}$ concentrations, the reaction goes to completion at both $TPB^{\ominus}$ concentrations; (b) Since the slopes of the plots are dependent only on the trityl ion concentrations present, the absorbances of the products obey Beer's Law and hence the absorbance is a valid measure of the concentration of the trityl ion/$TPB^{\ominus}$ complexes.

Notation

The rate constants, k, are subscripted by positive and negative numbers which respectively denote the forward and reverse rate constants for the corresponding step. The equilibrium constants, K, are subscripted with the corresponding step number.

Mechanism I

The first scheme considered,

Scheme V

$$[1]\quad RSO_3^{\ominus} \rightleftharpoons R^{\oplus}SO_3^{2\ominus}$$

$$[2a]\quad R^{\oplus}SO_3^{2\ominus} \rightleftharpoons R^{\oplus} + SO_3^{2\ominus}$$

$$[3a]\quad R^{\oplus} + TPB^{\ominus} \rightleftharpoons R^{\oplus}TPB^{\ominus}$$

$$[4]\quad R^{\oplus}TPB^{\ominus} + TPB^{\ominus} \longrightarrow R^{\oplus}(TPB^{\ominus})_2$$

is a simple S_N1 type involving free carbonium ion. The

first step, whereby the substrate forms an ion-pair prior to yielding kinetically free ions, is included for thoroughness. However, notice should be taken of the fact that the same dependence of the observed pseudo-first order rate constant on TPB^{θ} and $SO_3^{2\theta}$ concentrations will be obtained if steps [1] and [2a] of Scheme V are combined. (i.e. The substrate directly forms free ions.) Step [4] of Scheme V is considered to be irreversible and is justified by the observations discussed under Beer's Law. The expression for the observed rate constant is shown by*

$$[8] \quad k_{obs} = (k_1 k_{2a} k_{3a} k_4 [TPB^{\theta}]^2) / (k_{-1} k_{-2a} k_{-3a} [SO_3^{2\theta}] + (k_{-1} + k_{2a}) k_{3a} k_4 [TPB^{\theta}]^2 + k_{-1} k_{-2a} k_4 [SO_3^{2\theta}][TPB^{\theta}])$$

Inversion of Equation [8] produces

$$[9] \quad \frac{1}{k_{obs}} = \left(\frac{1}{K_1 K_{2a} K_{3a} k_4 [TPB^{\theta}]^2} + \frac{1}{K_1 K_{2a} k_{3a} [TPB^{\theta}]}\right)[SO_3^{2\theta}] + \frac{k_{-1} + k_{2a}}{k_1 k_{2a}}$$

This scheme produces a rate law which predicts that k_{obs}^{-1} should display a linear dependence on $SO_3^{2\theta}$ concentration at constant TPB^{θ} concentration, giving a positive slope de-

---

*See Appendix B for the derivation of pseudo-first order rate constant expressions.

pendent on TPB^{θ} concentration and a positive intercept independent of TPB^{θ} concentration. The dependence of k_{obs}^{-1} on $SO_3^{2\theta}$ concentration is clearly shown by the data (Figures 5 to 20, Tables 3 to 18) to be that predicted by Scheme V. The slopes, m, of the correlations of k_{obs}^{-1} with $SO_3^{2\theta}$ concentration at different TPB^{θ} concentrations are given by

$$[10] \quad m = \frac{1}{K_1 K_{2a} K_{3a} k_4 [TPB^{\theta}]^2} + \frac{1}{K_1 K_{2a} k_{3a} [TPB^{\theta}]}$$

which can be manipulated to give

$$[11] \quad m[TPB^{\theta}] = \frac{1}{K_1 K_{2a} K_{3a} k_4 [TPB^{\theta}]} + \frac{1}{K_1 K_{2a} k_{3a}}$$

Since all the constants in Equation [11] are necessarily positive, a correlation of $m[TPB^{\theta}]$ versus $[TPB^{\theta}]^{-1}$ must yield a positive slope and a positive intercept. The calculated data are reported in Tables 21 and 22 and the appropriate correlations are shown by Figures 21 and 22. The slopes of Figures 21 and 22 are obviously not positive and hence Scheme V does not yield physically acceptable results and cannot be an adequate description of the mechanism.

Mechanism II

The next scheme to be considered,

Table 21

$pMeOMGSO_3^{\theta}$ (fig. 21)

$[TPB^{\theta}]^a$	slope[b]	$[TPB^{\theta}]$slope[c]	$[TPB^{\theta}]^{-1}$ [d]
11.080	3.132	34.70	903
8.864	3.192	28.29	1128
6.650	4.555	30.29	1504
5.320	5.271	28.04	1880
4.433	4.526	20.06	2256
3.546	6.717	23.82	2820
2.660	8.147	21.67	3759
2.217	7.384	16.37	4511

units: (a) 10^{-4} M (b) 10^4 $M^{-1}s$ (c) s (d) M^{-1}

Reaction of $pMeOMGSO_3^{\ominus}$ with $TPB^{\ominus}$

Slope $[TPB^{\ominus}]$ —vs— $1/[TPB^{\ominus}]$

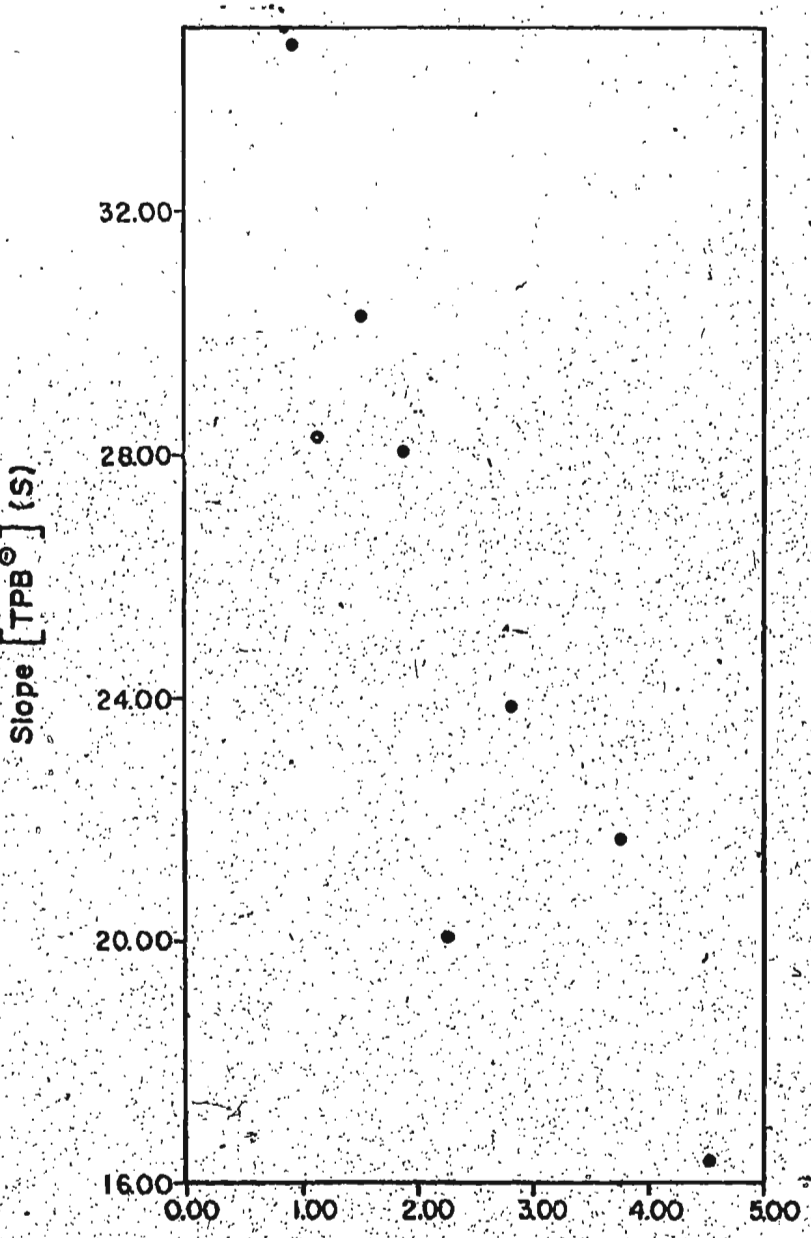

Fig. 21

Table 22

$MGSO_3^{\theta}$ (fig. 22)

$[TPB^{\theta}]^a$	slope[b]	$[TPB^{\theta}]$slope[c]	$[TPB^{\theta}]^{-1}$ [d]
11.335	2.298	260.5	882
9.068	2.650	240.3	1103
6.801	3.089	210.1	1470
5.441	3.584	195.0	1838
4.543	4.252	193.2	2201
3.634	3.984	145.7	2752
2.726	4.027	109.8	3668
2.272	4.819	109.5	4401

units: (a) 10^{-4} M (b) $10^5 M^{-1} s$ (c) s (d) M^{-1}

Reaction of $MGSO_3^{\ominus}$ with $TPB^{\ominus}$

Slope $\left[TPB^{\ominus}\right]$ —vs— $1/\left[TPB^{\ominus}\right]$

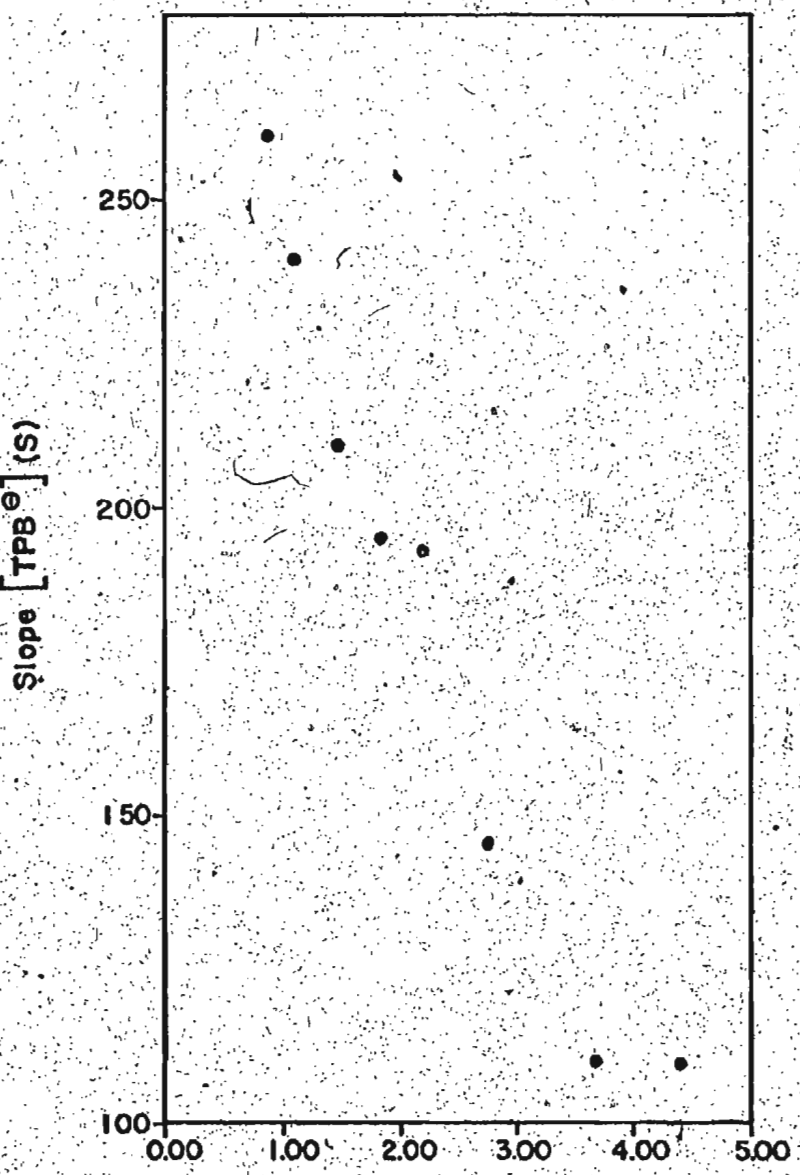

Fig. 22

Scheme VI

$$[1]\quad RSO_3^{\ominus} \rightleftharpoons R^{\oplus}SO_3^{2\ominus}$$

$$[2b]\quad R^{\oplus}SO_3^{2\ominus} + TPB^{\ominus} \rightleftharpoons TPB^{\ominus}R^{\oplus}SO_3^{2\ominus}$$

$$[3b]\quad TPB^{\ominus}R^{\oplus}SO_3^{2\ominus} \rightleftharpoons R^{\oplus}TPB^{\ominus} + SO_3^{2\ominus}$$

$$[4]\quad R^{\oplus}TPB^{\ominus} + TPB^{\ominus} \longrightarrow R^{\oplus}(TPB^{\ominus})_2$$

is an S_N2/ion-pair type, which does not involve free carbonium ion as in Scheme V. The expression for the observed rate constant is given by

$$[12]\quad k_{obs} = (k_1k_{2b}k_{3b}k_4[TPB^{\ominus}]^2) / (k_{-1}k_{-2b}k_{-3b}[SO_3^{2\ominus}] + k_{-1}(k_{-2b} + k_{3b})k_4[TPB^{\ominus}] + k_{2b}k_{3b}k_4[TPB^{\ominus}]^2)$$

Inversion of Equation [12] produces

$$[13]\quad \frac{1}{k_{obs}} = \frac{[SO_3^{2\ominus}]}{K_1K_{2b}K_{3b}k_4[TPB^{\ominus}]^2} + \frac{k_{-2b} + k_{3b}}{K_1k_{2b}k_{3b}[TPB^{\ominus}]} + \frac{1}{k_1}$$

Equation [13] predicts that k_{obs}^{-1} should plot as a linear function of $SO_3^{2\ominus}$ concentration at constant $TPB^{\ominus}$ concentration. This requirement has already been established. However, Scheme VI also requires that the intercepts of the k_{obs}^{-1} versus $SO_3^{2\ominus}$ concentration plots should be a function of $TPB^{\ominus}$ concentration, which conflicts with the observations. Equation [14]

$$[14]\quad m = \frac{1}{K_1K_{2b}K_{3b}k_4[TPB^{\ominus}]^2}$$

Table 23

$pMeOMGSO_3^{\ominus}$ (fig. 23)

$[TPB^{\ominus}]$ ($\times 10^{-4}$ M)	slope ($\times 10^{4}$ M^{-1} s)	$[TPB^{\ominus}]^{-2}$ ($\times 10^{5}$ M^{-2})
11.080	3.132	8.15
8.864	3.192	12.73
6.650	4.555	22.61
5.320	5.271	35.33
4.437	4.526	50.89
3.546	6.717	79.53
2.660	8.147	141.3
2.217	7.384	203.5

Reaction of pMeOMGSO$_3^{\ominus}$ with TPB$^{\ominus}$

Slopes —vs— $1/\left[TPB^{\ominus}\right]^2$

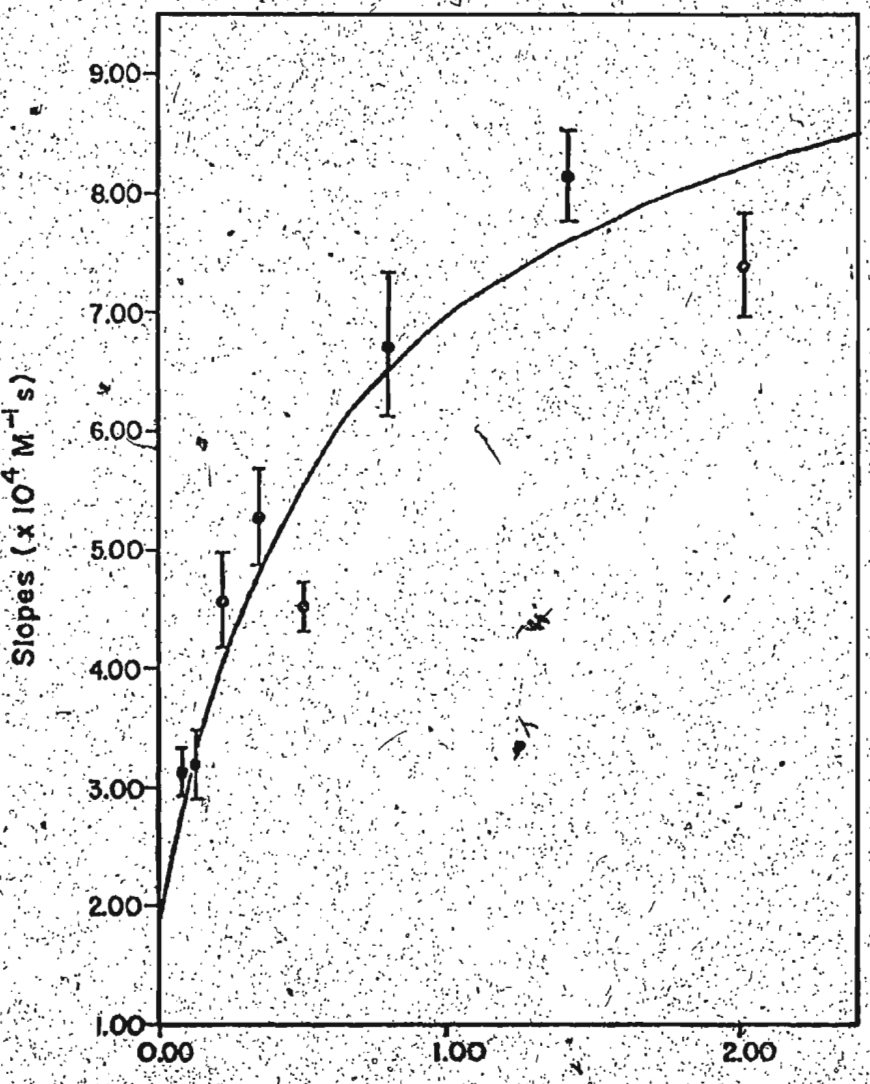

Fig. 23

Table 24

$MGSO_3^{\theta}$ (fig. 24)

$[TPB^{\theta}]$ ($\times 10^{-4}$ M)	slope ($\times 10^{5}$ M^{-1} s)	$[TPB^{\theta}]^{-2}$ ($\times 10^{5}$ M^{-2})
11.335	2.298	7.783
9.068	2.650	12.16
6.801	3.089	21.62
5.441	3.584	33.78
4.543	4.252	48.45
3.634	3.984	75.72
2.726	4.027	134.6
2.272	4.819	193.7

Reaction of $MGSO_3^{\ominus}$ with $TPB^{\ominus}$

Slopes –vs– $1/\left[TPB^{\ominus}\right]^2$

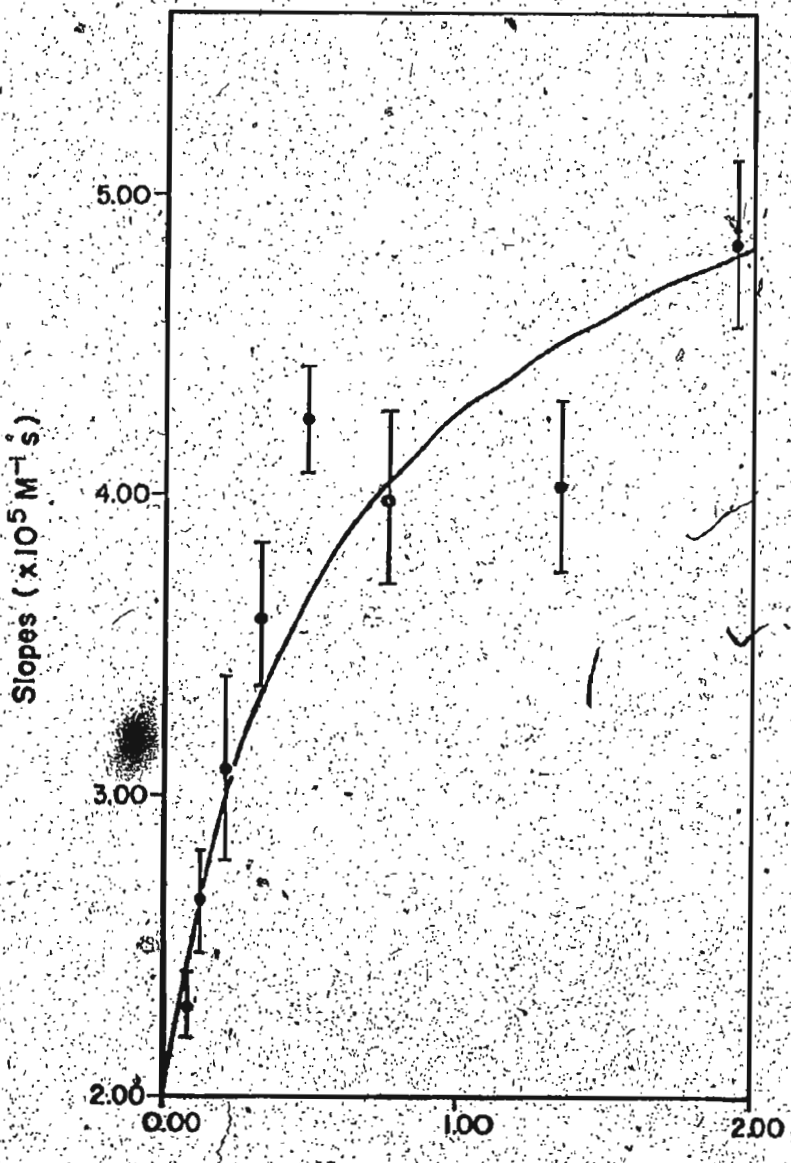

Fig. 24

provides an expression for the slopes, m, as a function of $TPB^{\ominus}$ concentration. Thus, the slopes should plot as a linear function of $[TPB^{\ominus}]^{-2}$. The calculated data are reported in Tables 23 and 24 and the appropriate correlations are presented in Figures 23 and 24. The plots are not linear and so Scheme VI, as already suspected, is not an adequate description of the mechanism.

Mechanism III

Schemes V and VI are partly correct; both predict the correct dependence of k_{obs}^{-1} on $SO_3^{2\ominus}$ concentration but neither Scheme V nor Scheme VI predicts the correct dependence of k_{obs} on $TPB^{\ominus}$ concentration. Since the attack of $TPB^{\ominus}$ directly on the trityl ion is known to be very rapid, possibly Schemes V and VI include steps after the rate determining step. Based on the knowledge of the rapidity of $TPB^{\ominus}$ attack on the free trityl ions, the formation of the product from the $R^{\oplus}TPB^{\ominus}$ ion-pair in both Schemes V and VI should be extremely rapid. Therefore, the formation of $R^{\oplus}TPB^{\ominus}$ is possibly the rate determining step of the reaction.

The next scheme to be considered,

Scheme VII

$$[1]\quad RSO_3^{\ominus} \rightleftharpoons R^{\oplus}SO_3^{2\ominus}$$

$$[2a]\quad R^{\oplus}SO_3^{2\ominus} \rightleftharpoons R^{\oplus} + SO_3^{2\ominus}$$

$$[3a]\quad R^{\oplus} + TPB^{\ominus} \longrightarrow R^{\oplus}TPB^{\ominus}$$

is an abbreviated form of Scheme V. In this scheme, the final conversion of the ion-pair, $R^{\oplus}TPB^{\ominus}$, to the ion-triplet, $R^{\oplus}(TPB^{\ominus})_2$, is considered to be very rapid and irreversible. Therefore, step 3a of Scheme VII is now irreversible. Equation [15]

$$[15] \quad k_{obs} = \frac{k_1 k_{2a} k_{3a} [TPB^{\ominus}]}{(k_{-1} + k_{2a}) k_{3a} [TPB^{\ominus}] + k_{-1} k_{-2a} [SO_3^{2\ominus}]}$$

is now the expression for the observed rate constant. After the usual manipulation, Equation [15] yields

$$[16] \quad \frac{1}{k_{obs}} = \frac{[SO_3^{2\ominus}]}{K_1 K_{2a} k_{3a} [TPB^{\ominus}]} + \frac{k_{-1} + k_{2a}}{k_1 k_{2a}}$$

Equation [16] predicts the same dependence of k_{obs} on $SO_3^{2\ominus}$ concentration established earlier with constant intercepts as both the $SO_3^{2\ominus}$ and $TPB^{\ominus}$ concentrations are varied. The slopes, m, of the k_{obs}^{-1} versus $SO_3^{2\ominus}$ concentration correlations, given by

$$[17] \quad m = \frac{1}{K_1 K_{2a} k_{3a} [TPB^{\ominus}]}$$

should be linearly dependent on the reciprocal of the $TPB^{\ominus}$ concentration with a zero intercept. The calculated data relevant to Equation [17] are given in Tables 25 and 26, and the related correlations (m versus $[TPB^{\ominus}]^{-1}$) in Figures 25 and 26. Although the slopes do appear to be linear versus

Table 25

$pMeOMGSO_3^{\ominus}$ (fig. 25)

$[TPB^{\ominus}]$ ($\times 10^{-4}$ M)	slope ($\times 10^{4}$ M^{-1} s)	$[TPB^{\ominus}]^{-1}$ ($\times 10^{5}$ M^{-2})
11.080	3.132	903
8.864	3.192	1128
6.650	4.555	1504
5.320	5.271	1880
4.433	4.526	2256
3.546	6.717	2820
2.660	8.147	3759
2.217	7.384	4511

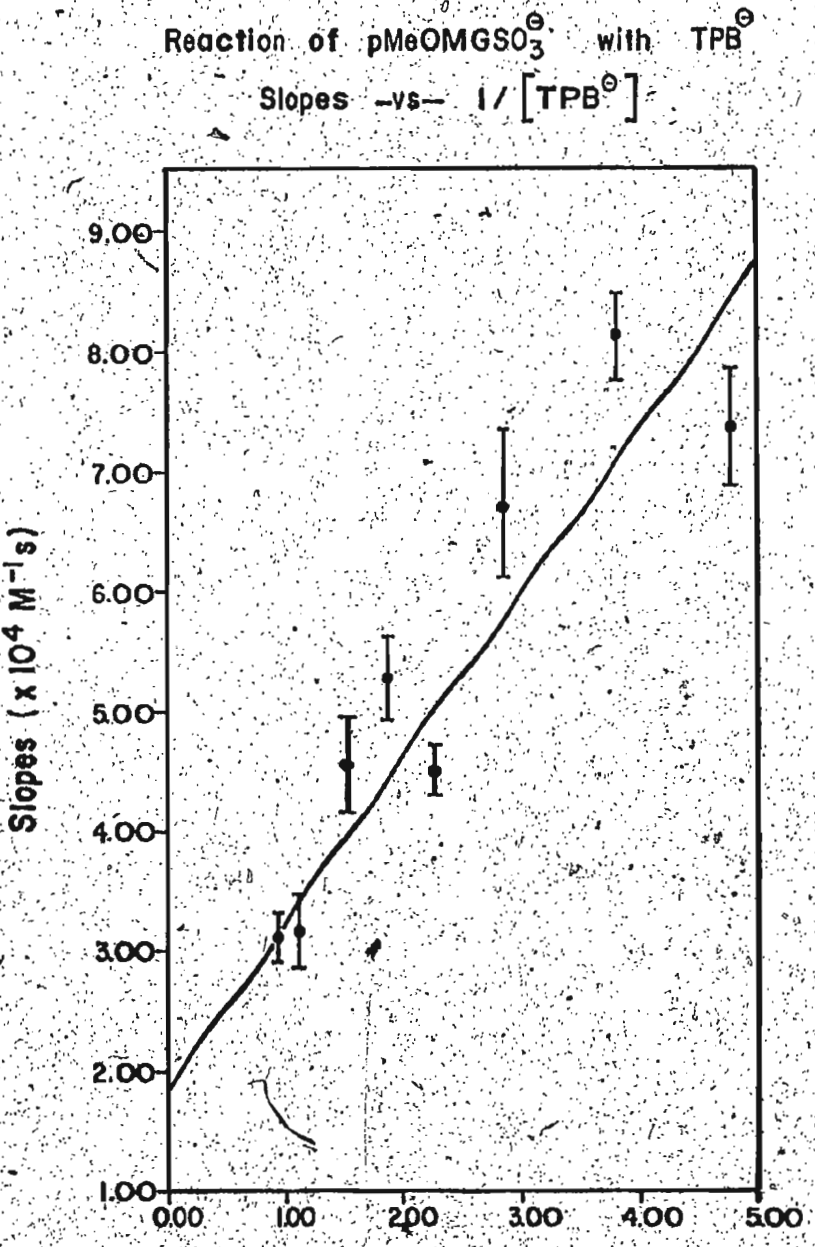
Reaction of pMeOMGSO3⊖ with TPB⊖
Slopes -vs- 1/[TPB⊖]
Slopes (x10⁴ M⁻¹s)
9.00
8.00
7.00
6.00
5.00
4.00
3.00
2.00
1.00
0.00
1.00
2.00
3.00
4.00
5.00
1/[TPB⊖] (x10³ M⁻¹)

Fig. 25

Table 26

$MGSO_3^{\theta}$ (fig. 26)

$[TPB^{\theta}](\times 10^{-4}M)$	slope$(\times 10^{5}M^{-1}s)$	$[TPB^{\theta}]^{-1}(\times 10^{5}M^{-2})$
11.335	2.298	882
9.068	2.650	1108
6.801	3.089	1470
5.441	3.584	1838
4.543	4.252	2201
3.634	3.984	2752
2.726	4.027	3668
2.272	4.819	4401

Reaction of $MGSO_3^{\ominus}$ with $TPB^{\ominus}$

Slopes -vs- $1/[TPB^{\ominus}]$

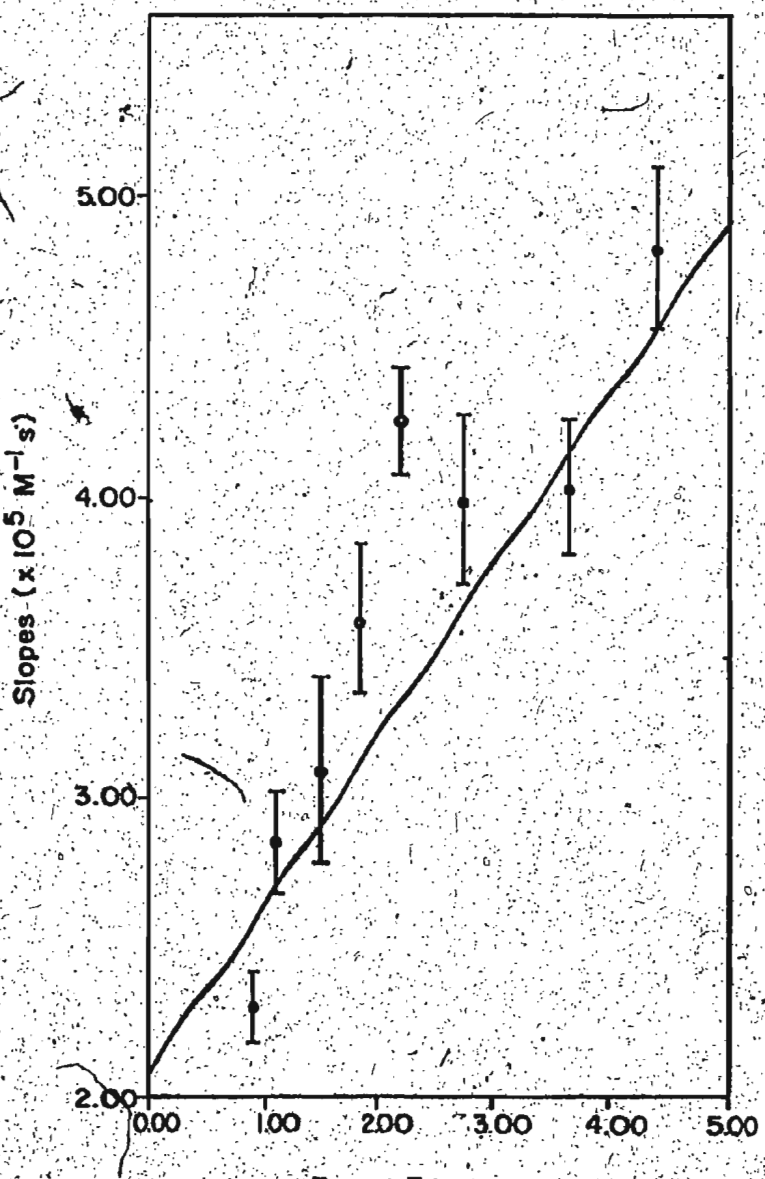

Fig. 26

reciprocal $TPB^{\ominus}$ concentration, the intercepts are far from zero. Therefore, Scheme VII is also an inadequate description of the mechanism.

Mechanism IV

The next scheme,

Scheme VIII

$$[1]\quad RSO_3^{\ominus} \rightleftharpoons R^{\bullet}SO_3^{2\ominus}$$

$$[2b]\quad R^{\bullet}SO_3^{2\ominus} + TPB^{\ominus} \rightleftharpoons TPB^{\ominus}R^{\bullet}SO_3^{2\ominus}$$

$$[3b]\quad TPB^{\ominus}R^{\bullet}SO_3^{2\ominus} \longrightarrow R^{\bullet}TPB^{\ominus} + SO_3^{2\ominus}$$

is a truncated version of Scheme VI. The final coversion of the ion-pair, $R^{\bullet}TPB^{\ominus}$, to the ion-triplet, $R^{\bullet}(TPB^{\ominus})_2$, is considered to be very rapid and irreversible, which now makes step 3b of Scheme VIII irreversible. Without any further discussion, Scheme VIII quite obviously predicts k_{obs} to be independent of $SO_3^{2\ominus}$ concentration and so is inconsistent with the experimental results.

Mechanism V

The next scheme to be considered,

Scheme IX

$$[1]\quad RSO_3^{\ominus} \rightleftharpoons R^{\bullet}SO_3^{2\ominus}$$

$$[2a]\quad R^{\bullet}SO_3^{2\ominus} \rightleftharpoons R^{\bullet} + SO_3^{2\ominus}$$

$$[2b]\quad R^{\bullet}SO_3^{2\ominus} + TPB^{\ominus} \rightleftharpoons TPB^{\ominus}R^{\bullet}SO_3^{2\ominus}$$

$$[3a]\quad R^{\bullet} + TPB^{\ominus} \longrightarrow R^{\bullet}TPB^{\ominus}$$

$$[3b]\quad TPB^{\ominus}R^{\ominus}SO_3^{2\ominus} \longrightarrow R^{\ominus}TPB^{\ominus} + SO_3^{2\ominus}$$

is a hybrid of Schemes VII and VIII. Again, the final conversion of the ion-pair, $R^{\ominus}TPB^{\ominus}$, to ion-triplet, $R^{\ominus}(TPB^{\ominus})_2$, is considered to be rapid and irreversible which makes steps 3a and 3b of Scheme IX irreversible. The expression for the observed rate constant is given by

$$[18]\quad k_{obs} = \{k_1k_{2a}k_{3a}(k_{-2b} + k_{3b})[TPB^{\ominus}] + k_1k_{2b}k_{3b}(k_{-2a}[SO_3^{2\ominus}] + k_{3a}[TPB^{\ominus}])[TPB^{\ominus}])\ /$$
$$\{k_{-2a}k_{2b}k_{3b}[TPB^{\ominus}][SO_3^{2\ominus}] + (k_{-1} + k_{2a})(k_{-2b} + k_{3b})k_{3a}[TPB^{\ominus}] + k_{-1}k_{-2a}(k_{-2b} + k_{3b})[SO_3^{2\ominus}] + k_{2b}k_{3a}k_{3b}[TPB^{\ominus}]^2\}$$

Equation [18] is complex but can be simplified. Since the concentrations used for $SO_3^{2\ominus}$ are of the order 10^{-3}M and the $TPB^{\ominus}$ concentrations are of the order 10^{-4}M, terms involving either $[TPB^{\ominus}]$ or $[TPB^{\ominus}][SO_3^{2\ominus}]$ should be negligibly small, depending on the values of the rate constants. Taking note of the already observed rapid attack of $SO_3^{2\ominus}$ and the more rapid attack of $TPB^{\ominus}$ on the free trityl ion, the coefficients of the $[TPB^{\ominus}]$, $[TPB^{\ominus}]^2$ and $[TPB^{\ominus}][SO_3^{2\ominus}]$ terms in the numerator are probably of approximately the same order of magnitude. In the denominator, the coefficients of the $[TPB^{\ominus}]$, $[TPB^{\ominus}]^2$ and $[SO_3^{2\ominus}]$ terms are probably of approximately the same order of magnitude. The coefficient of the

$[TPB^{\theta}][SO_3^{2\theta}]$ term in the denominator is probably significantly larger than the other coefficients in the denominator. Therefore, in the concentration ranges used in this study, the $[TPB^{\theta}][SO_3^{2\theta}]$ and $[TPB^{\theta}]^2$ terms in the numerator are probably negligible and the $[TPB^{\theta}]^2$ term in the denominator is probably negligible. Now Equation [18] can be simplified to

$$[19] \quad k_{obs} = (k_1 k_{2a} k_{3a} (k_{-2b} + k_{3b})[TPB^{\theta}]) / (k_{-2a} k_{2b} k_{3b}[TPB^{\theta}][SO_3^{2\theta}] + (k_{-1} + k_{2a})(k_{-2b} + k_{3b}) k_{3a}[TPB^{\theta}] + k_{-1} k_{-2a} (k_{-2b} + k_{3b})[SO_3^{2\theta}])$$

By the usual manipulation and then factoring,

$$[20] \quad \frac{1}{k_{obs}} = \left(\frac{1}{K_1 K_{2a} k_{3a} [TPB^{\theta}]} + \frac{k_{2b} k_{3b}}{k_1 K_{2a} k_{3a} (k_{-2b} + k_{3b})}\right)[SO_3^{2\theta}] + \frac{k_{-1} + k_{2a}}{k_1 k_{2a}}$$

is obtained from Equation [19]. Again, Equation [20] predicts the same dependence of k_{obs} on $SO_3^{2\theta}$ concentration as already established. Equation [21]

$$[21] \quad m = \frac{1}{K_1 K_{2a} k_{3a} [TPB^{\theta}]} + \frac{k_{2b} k_{3b}}{k_1 K_{2a} k_{3a} (k_{-2b} + k_{3b})}$$

gives an expression for the dependence of the slopes, m, of the k_{obs}^{-1} versus $SO_3^{2\theta}$ concentration plots on TPB^{θ} concentra-

tion. According to Equation [21], the slopes should be linearly dependent on reciprocal $TPB^{\ominus}$ concentration with a positive intercept. This dependence of the slopes on $TPB^{\ominus}$ concentration is supported by the calculated data given in Tables 25 and 26, and the correlations, Figures 25 and 26, pages 75 to 78.

Mechanism VI

Before accepting Scheme IX as an adequate description of the mechanism, the necessity of all the intermediates must be discussed. Because of the presence of the large phenyl groups on both the $TPB^{\ominus}$ ion and the trityl group, direct attack of $TPB^{\ominus}$ on $RSO_3^{\ominus}$ is sterically hindered. Therefore, $TPB^{\ominus}$ is unlikely to attack an un-ionized form of $RSO_3^{\ominus}$ and so the inclusion of the species $R^{\bullet}SO_3^{2\ominus}$ in the scheme is necessary. The problem now is whether or not the inclusion of the $TPB^{\ominus}R^{\bullet}SO_3^{2\ominus}$ species is necessary. The exclusion of this asymmetric triplet species is equivalent to the combining of steps 2b and 3b of Scheme IX to give

Scheme X

$$[1] \quad RSO_3^{\ominus} \rightleftharpoons R^{\bullet}SO_3^{2\ominus}$$

$$[2a] \quad R^{\bullet}SO_3^{2\ominus} \rightleftharpoons R^{\bullet} + SO_3^{2\ominus}$$

$$[3a] \quad R^{\bullet} + TPB^{\ominus} \rightleftharpoons R^{\bullet}TPB^{\ominus}$$

$$[2b3b] \quad R^{\bullet}SO_3^{2\ominus} + TPB^{\ominus} \longrightarrow R^{\bullet}TPB^{\ominus} + SO_3^{2\ominus}$$

The expression for the observed rate constant is given by

$$[22] \quad k_{obs} = (k_1 k_{-2a} k_{2b3b} [TPB^{\theta}][SO_3^{2\theta}] + k_1 k_{2b3b} k_{3a} [TPB^{\theta}]^2 + k_1 k_{2a} k_{3a} [TPB^{\theta}]) / (k_{-1} k_{-2a} [SO_3^{2\theta}] + (k_{-1} + k_{2a}) k_{3a} [TPB^{\theta}] + k_{-2a} k_{2b3b} [TPB^{\theta}][SO_3^{2\theta}] + k_{2b3b} k_{3a} [TPB^{\theta}]^2)$$

Equation [22] can be simplified in the same way and for the same reasons as Equation [18] to give

$$[23] \quad k_{obs} = (k_1 k_{2a} k_{3a} [TPB^{\theta}]) / (k_{-1} k_{-2a} [SO_3^{2\theta}] + (k_{-1} + k_{2a}) k_{3a} [TPB^{\theta}] + k_{-2a} k_{2b3b} [TPB^{\theta}][SO_3^{2\theta}])$$

By inverting Equation [23],

$$[24] \quad \frac{1}{k_{obs}} = \left(\frac{1}{K_1 K_{2a} k_{3a} [TPB^{\theta}]} + \frac{k_{2b3b}}{k_1 K_{2a} k_{3a}}\right)[SO_3^{2\theta}] + \frac{k_{-1} + k_{2a}}{k_1 k_{2a}}$$

is obtained. The expression for the slopes, m, of the k_{obs}^{-1} versus $SO_3^{2\theta}$ concentration is shown by

$$[25] \quad m = \frac{1}{K_1 K_{2a} k_{3a} [TPB^{\theta}]} + \frac{k_{2b3b}}{k_1 K_{2a} k_{3a}}$$

Thus, Schemes IX and X predict exactly the same form of the dependence of k_{obs} on $SO_3^{2\theta}$ and TPB^{θ} concentrations. There is no operational difference between Schemes IX and X; the

only difference is the interpretation of the intercept terms of the slopes correlated with reciprocal TPB^{θ} concentration.

Conclusion

The description of the mechanism of the reaction studied in this work must include the reversible ionization of $SO_3^{2\ominus}$ from the trityl group. This ionization most probably occurs via the Winstein scheme (Scheme III), leaving many different species of solvent separated ion-pairs open to possible attack by $TPB^{\ominus}$. Simply just considering attack of $TPB^{\ominus}$ on the kinetically free trityl ion (Scheme VII) produces a rate law which closely describes the data except for predicting a zero intercept on the slopes versus reciprocal $TPB^{\ominus}$ concentration correlation. Therefore, the consideration of the attack of $TPB^{\ominus}$ on an intermediate in the Winstein scheme is necessary. Because of the rapidity of the reaction of $SO_3^{2\ominus}$ with the free trityl ions, the most abundant of the ion-pair species is the intimate ion-pair and so this species is the intermediate of the Winstein scheme most likely to be involved. According to the data, there is no evidence to support the presence of the $TPB^{\ominus}R^{\oplus}SO_3^{2\ominus}$ species; however, neither is its presence refuted. Because of the high affinity of both $TPB^{\ominus}$ and $SO_3^{2\ominus}$ for the trityl ions and the evidence for the existence of the ion-triplet, $R^{\oplus}(TPB^{\ominus})_2$, as the product, the presence of the $TPB^{\ominus}R^{\oplus}SO_3^{2\ominus}$ species is quite possible.

Finally, the data were fitted to

$$[26] \quad k_{obs}^{-1} = (m_2[TPB^{\ominus}]^{-1} + b_2)[SO_3^{2\ominus}] + b_1$$

$$m_2 = \frac{1}{K_1 K_{2a} k_{3a}}$$

$$b_2 = \frac{k_{2b} k_{3b}}{k_1 K_{2a} k_{3a} (k_{-2b} + k_{3b})} \quad \text{(Scheme IX)}$$

$$b_2 = \frac{k_{2b3b}}{k_1 K_{2a} k_{3a}} \quad \text{(Scheme X)}$$

$$b_1 = \frac{k_{-1} + k_{2a}}{k_1 k_{2a}}$$

which is derived from either of Equations [20] or [24], by the Wentworth algorithm (28) and the best values for m_2, b_2, and b_1 are obtained. For this calculation, which requires errors for all variables, the errors used on the concentrations are all ±5 in the last decimal place cited and the errors used on the observed rate constants are those calculated from the raw data. The results of this curve fit are shown in Table 27. The only comment on the derived values for the parameters of Equation [26] is simply that, as expected, the dissociation of $SO_3^{2\ominus}$ from $MG^{\bullet}$ is slower than that from $pMeOMG^{\bullet}$ ($b_1^{-1} = 3.43 \times 10^{-3} s^{-1}$ and $9.17 \times 10^{-3} s^{-1}$ respectively). The rates of displacement of $SO_3^{2\ominus}$ by $TPB^{\ominus}$ are evidently faster on $pMeOMG^{\bullet}$ than on $MG^{\bullet}$, also as expected, because of the stablizing influence of the methoxy group on $pMeOMG^{\bullet}$ that is not present on $MG^{\bullet}$. Ritchie (28) claims that the equilibrium constant for the association of

Table 27 Wentworth general regression analysis:

$pMeOMGSO_3^{2\ominus}$:

$m_2 = 13.99 \pm 0.10$ s

$b_2 = 1.876 \pm 0.023 \times 10^4 M^{-1}s$

$b_1 = 109.1 \pm 0.7$ s

Covariances:

$m_2,b_2 = -15.88\ M^{-1}s^2$

$m_2,b_1 = -1.306 \times 10^{-4}s^2$

$b_2,b_1 = -102.5\ M^{-1}s^2$

$MGSO_3^{2\ominus}$:

$m_2 = 59.00 \pm 0.97$ s

$b_2 = 2.269 \pm 0.025 \times 10^5 M^{-1}s$

$b_1 = 291.2 \pm 4.7$ s

Covariances:

$m_2,b_2 = -1699\ M^{-1}s^2$

$m_2,b_1 = -0.02438\ s^2$

$b_2,b_1 = -7490\ M^{-1}s^2$

$MG^{\oplus}$ with $SO_3^{2\ominus}$ is greater than $10^6\ M^{-1}$. Given Scott's data (21) for the forward rate of the reaction ($4.47 \times 10^3 M^{-1}s^{-1}$) and the reverse rate reported here the equilibrium constant is $1.30 \times 10^6 M^{-1}$ which agrees with Ritchie's claim.

Practical Limitations

In order to place this work in its proper perspective, an account must be made of the practical limitations involved in the experimental research. Because of the low solubilities of the trityl ions used and NaTPB, the highest concentrations possible are limited. The trityl ion concentrations are further limited by the range in which the absorbance changes follow Beer's Law. The lowest $TPB^{\ominus}$ concentration must be great enough to ensure pseudo-first order kinetics. Thus, the possible concentration range is limited and the product determination is restricted to deduction from the kinetics of the reaction.*

Since $TPB^{\ominus}$ is capable of displacing $SO_3^{2\ominus}$ on trityl ions, the equilibrium constant for the association of $TPB^{\ominus}$ with the trityl ions must be larger than the corresponding equilibrium constant for $SO_3^{2\ominus}$. Thus, the equilibrium constant for the association of $TPB^{\ominus}$ with the trityl ions is

---

*In the literature concerning the reactions of trityl ions, there is a marked absence of product determination because of the low concentrations used. In the reactions between trityl ions and amines, there is debate over whether the product is the amine or carbinol (29).

impossibly large to measure directly just as the measurement of the equilibrium constant for $SO_3^{2\ominus}$ with some of the trityl ions can, at present, only be measured through displacement by $TPB^{\ominus}$. The measurement of the overall equilibrium constant for the displacement of $SO_3^{2\ominus}$ by $TPB^{\ominus}$, is also presently impossible to determine. As already noted, the reaction goes to completion at the concentrations used. If the $TPB^{\ominus}$ concentration be dropped to allow an equilibrium study, the possibility of the formation of another ionic species, $(R^{\ominus})_2TPB^{\ominus}$, must be considered which further complicates the system. Also, at these low $TPB^{\ominus}$ concentrations the absorbance changes are small and useful information is extremely difficult to obtain.

Another limitation is the lack of stablity of the $SO_3^{2\ominus}$ ion in aqueous solution. Thus, every run must be prepared from a fresh sample of dry Na_2SO_3 which disallows any two runs to be run with identical concentrations. Therefore, reproducibility of results can only be determined by how well the data fit the derived rate law in the final analysis.

Finally, there is a limitation on the presentation of the data. The observed rate constant is a function of two variables which is difficult to adequately represent on a two dimensional graph. This restriction necessitates the removal of one variable by making it constant. The $TPB^{\ominus}$ concentrations are kept constant for a series of $SO_3^{2\ominus}$ con-

centrations. An important point to note is that the solutions are prepared individually and so the 'constant' $TPB^{\ominus}$ concentrations actually involve measurement errors. Since the rate of attack of $TPB^{\ominus}$ on the trityl ions is very rapid, small errors in the $TPB^{\ominus}$ concentrations may make the correlation of k_{obs}^{-1} with $SO_3^{2\ominus}$ concentration appear poor. However, this problem is largely overcome by using the Wentworth algorithm to determine the parameters of the derived rate law.

Implications

The obvious extension of the current work is to use this reaction to determine the large equilibrium constants for the association of certain nucleophiles with certain trityl ions. Another interesting study is the effect of solvent on this reaction. As noted, $TPB^{\ominus}$ will displace $SO_3^{2\ominus}$ in water but not in acetone. Various solvents and solvent mixtures will give more insight into the nature of the ionic association between the trityl ions and $TPB^{\ominus}$. Finally, another area which requires investigation is the effect the stability of the trityl ion involved has on the ability of $TPB^{\ominus}$ to replace nucleophiles.

This reaction also has important implications for nucleophilic attack on the trityl ions specifically and nucleophilic substitution in general. This work suggests that ion-pair formation is very rapid and the possibility of

rapid ion-pair formation, with the further possibility of ion-triplet formation, prior to covalent bond formation should be thoroughly investigated. By considering a more complex mechanism for nucleophilic attack on the trityl ions, the apparent anomalies in the literature data may be eliminated.

Appendix A

The data sets presented in this appendix are two examples of the raw data, one for each trityl ion studied. These data demonstrate the adherence to pseudo-first order kinetics except for the slight deviation of the first two points, which, if included, produce a lower value for the observed rate constant. Assuming the formation of the ion triplet, $R^{\oplus}(TPB^{\ominus})_2$, as the product, the initial rate of formation of product will be nil due to there initially being no ion pair, $R^{\oplus}TPB^{\ominus}$, present. Thus, during the induction period, the observed rate constant will be lower, as noted, until steady state is achieved, with a resulting adherence to pseudo-first order kinetics.

Table 28

Sample first order data: $pMeOMGSO_3^{\ominus}$ (Fig. 27)

$[TPB^{\ominus}] = 4.433 \times 10^{-4}M$ $[SO_3^{2\ominus}] = 1.93 \times 10^{-3}M$

time (s)	P	$P_i - P$	$\ln(P_i - P)$
30.0	0.073	0.391	-0.940
60.0	0.114	0.350	-1.050
90.0	0.158	0.305	-1.186
120.0	0.196	0.268	-1.318
150.0	0.231	0.232	-1.461
180.0	0.260	0.203	-1.594
210.0	0.291	0.173	-1.756
240.0	0.314	0.149	-1.903
270.0	0.332	0.132	-2.026
300.0	0.350	0.114	-2.174
330.0	0.367	0.097	-2.334
360.0	0.379	0.085	-2.470
390.0	0.389	0.074	-2.602
420.0	0.400	0.063	-2.759
450.0	0.409	0.055	-2.909
480.0	0.417	0.047	-3.065
510.0	0.423	0.041	-3.196
540.0	0.428	0.035	-3.348
570.0	0.433	0.031	-3.491

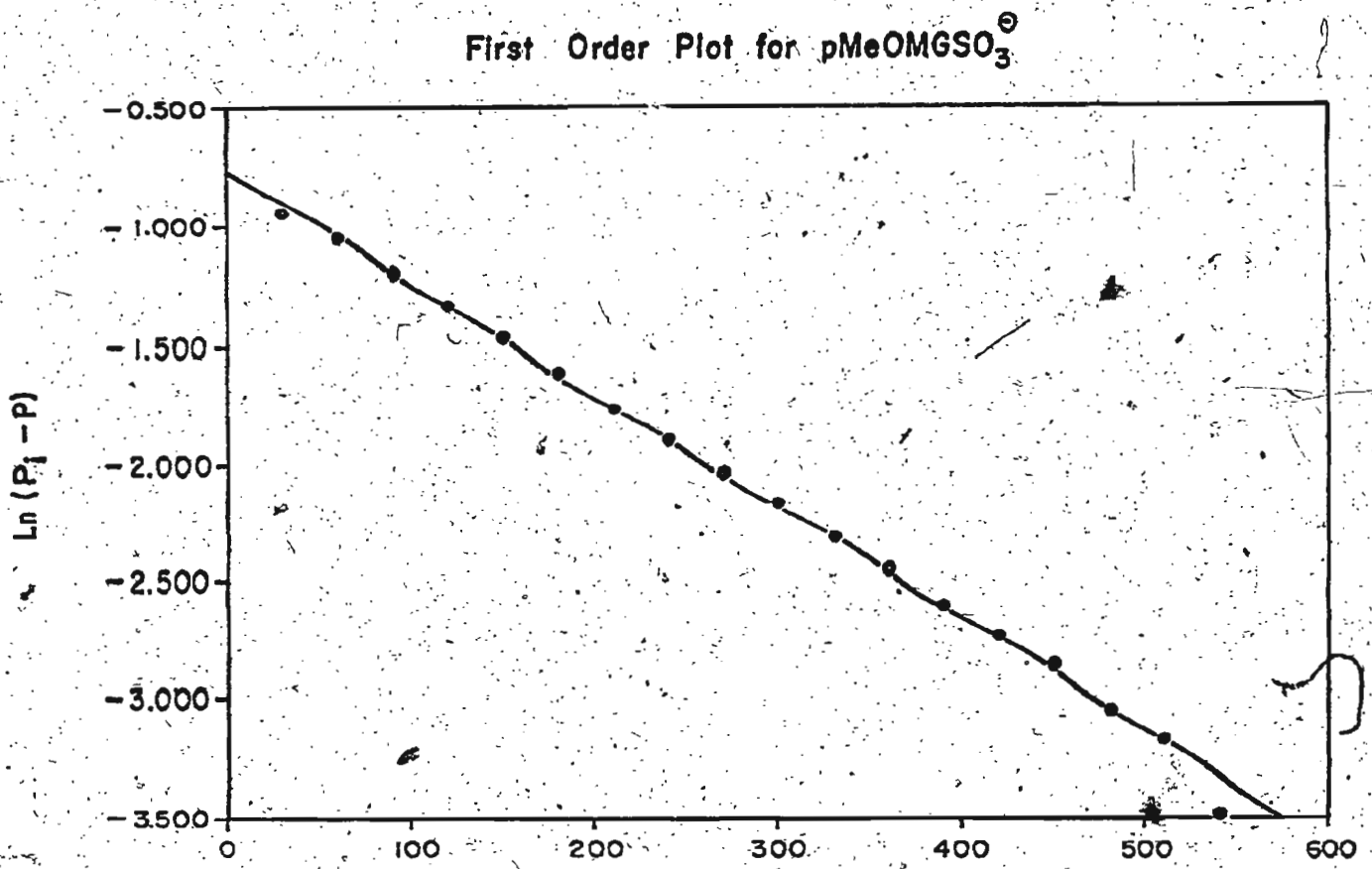
First Order Plot for pMeOMGSO3⊖
-0.500
-1.000
-1.500
-2.000
-2.500
-3.000
-3.500
Ln (P∞ - P)
0
100
200
300
400
500
600
t (s)

Fig. 27

Table 29

Sample first order data: $MGSO_3^{\theta}$ (fig. 28)

$[TPB^{\theta}] = 4.543 \times 10^{-4} M$ $[SO_3^{2\theta}] = 3.54 \times 10^{-3} M$

time (s)	P	$P_i - P$	$\ln(P_i - P)$
119.1	0.012	0.548	-0.601
238.2	0.036	0.525	-0.644
357.3	0.062	0.499	-0.695
476.4	0.087	0.473	-0.748
595.5	0.112	0.448	-0.802
714.6	0.140	0.421	-0.865
833.7	0.164	0.397	-0.924
952.8	0.187	0.374	-0.985
1071.9	0.209	0.352	-1.045
1191.0	0.233	0.328	-1.115
1310.1	0.254	0.307	-1.182
1429.2	0.277	0.284	-1.258

Table 29 (cont'd)

time (s)	P	$P_i - P$	$\ln(P_i - P)$
1548.3	0.298	0.263	-1.335
1667.4	0.312	0.249	-1.390
1786.5	0.327	0.234	-1.454
1905.6	0.343	0.218	-1.525
2024.7	0.355	0.206	-1.579
2143.8	0.367	0.194	-1.639
2262.9	0.378	0.183	-1.699
2382.0	0.388	0.172	-1.758
2501.1	0.401	0.160	-1.836
2620.2	0.412	0.148	-1.908
2739.3	0.420	0.141	-1.963
2858.4	0.424	0.137	-1.988

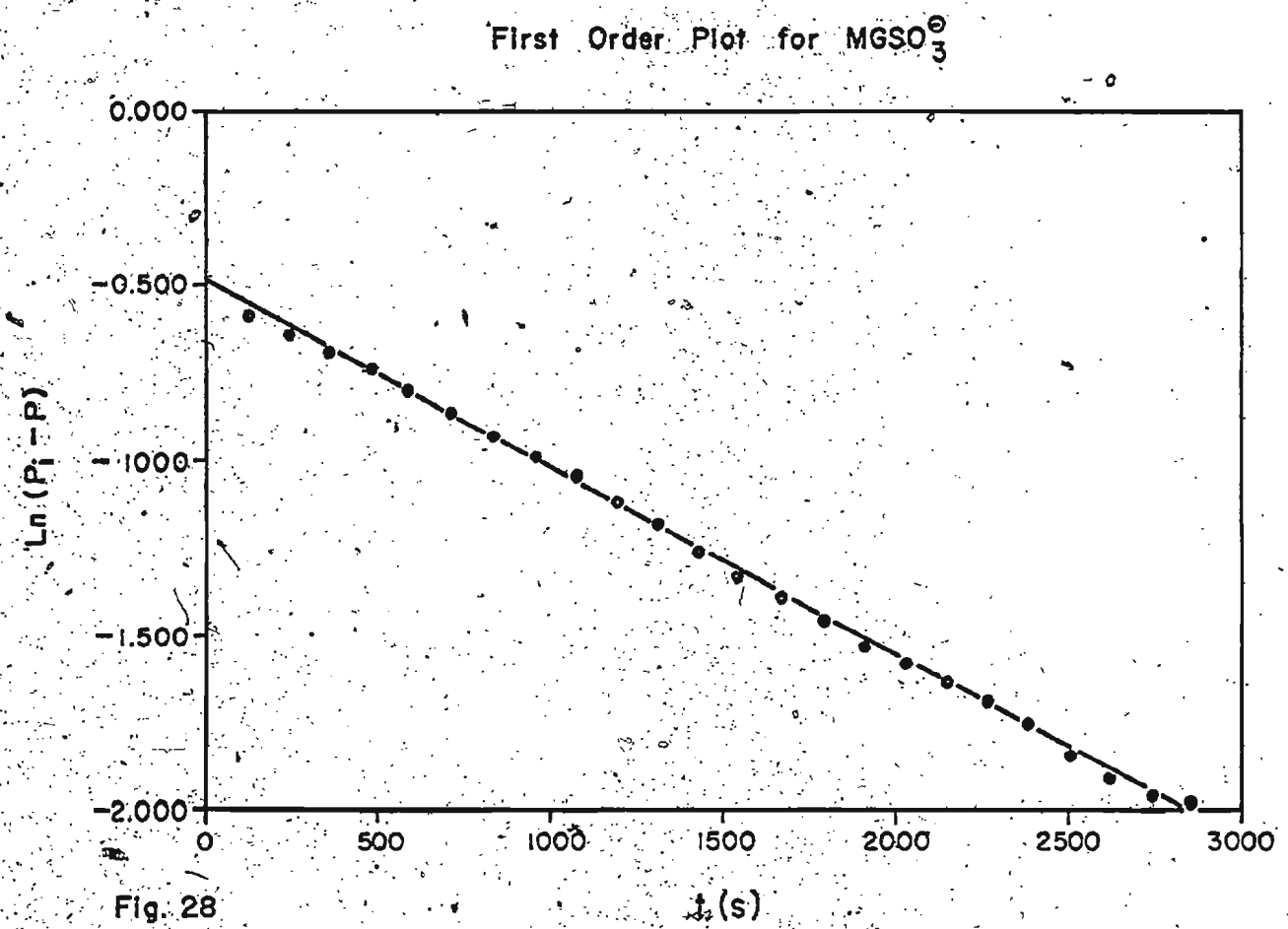
First Order Plot for $MGSO_3^{\ominus}$
0.000
-0.500
-1.000
-1.500
-2.000
Ln $(P_i - P)$
0
500
1000
1500
2000
2500
3000
$t_{\frac{1}{2}}$ (s)

Fig. 28

Appendix B

In the following derivations of rate laws, some of the equations cited also appear in the main body of the text. When this occurs, the number of the equation in the main body of the text is indicated after the equation.

All the schemes cited use a selection of the following steps:

[1] $RSO_3^{\ominus} \rightleftharpoons R^{\oplus}SO_3^{2\ominus}$

[2a] $R^{\oplus}SO_3^{2\ominus} \rightleftharpoons R^{\oplus} + SO_3^{2\ominus}$

[3a] $R^{\oplus} + TPB^{\ominus} \rightleftharpoons R^{\oplus}TPB^{\ominus}$

[2b] $R^{\oplus}SO_3^{2\ominus} + TPB^{\ominus} \rightleftharpoons TPB^{\ominus}R^{\oplus}SO_3^{2\ominus}$

[3b] $TPB^{\ominus}R^{\oplus}SO_3^{2\ominus} \rightleftharpoons R^{\oplus}TPB^{\ominus} + SO_3^{2\ominus}$

[4] $R^{\oplus}TPB^{\ominus} + TPB^{\ominus} \longrightarrow R^{\oplus}(TPB^{\ominus})_2$

For convenience and clarity, the steps are always numbered the same way, no matter in which scheme they are used. In all cases, the scheme is first stated. Next, the differential equations related to the steady state are given followed by a summary of the steady state in matrix notation. The expressions for the observed rate and observed pseudo-first order rate constant are now stated. Finally, the observed pseudo-first order is expressed in terms of single step rate constants and $SO_3^{2\ominus}$ and $TPB^{\ominus}$ concentrations.

A summary of the set of steps used in each scheme is as follows:

	1	2a	3a	2b	3b	4
Scheme V	x	x	x			x
Scheme VI	x			x	x	x
Scheme VII	x	x	x			
Scheme VIII	x			x	x	
Scheme IX	x	x	x	x	x	
Scheme X	x	x	x	combined		

Scheme V

$$[1]\quad RSO_3^{\ominus} \rightleftharpoons R^{\bullet}SO_3^{2\ominus}$$

$$[2a]\quad R^{\bullet}SO_3^{2\ominus} \rightleftharpoons R^{\bullet} + SO_3^{2\ominus}$$

$$[3a]\quad R^{\bullet} + TPB^{\ominus} \rightleftharpoons R^{\bullet}TPB^{\ominus}$$

$$[4]\quad R^{\bullet}TPB^{\ominus} + TPB^{\ominus} \longrightarrow R^{\bullet}(TPB^{\ominus})_2$$

Steady state equations:

$$[27]\quad \frac{d[R^{\bullet}SO_3^{2\ominus}]}{dt} = k_1[RSO_3^{\ominus}] - (k_{-1} + k_{2a})[R^{\bullet}SO_3^{2\ominus}] + k_{-2a}[R^{\bullet}][SO_3^{2\ominus}] = 0$$

$$[28]\quad \frac{d[R^{\bullet}]}{dt} = k_{2a}[R^{\bullet}SO_3^{2\ominus}] - (k_{-2a}[SO_3^{2\ominus}] + k_{3a}[TPB^{\ominus}])[R^{\bullet}] + k_{-3a}[R^{\bullet}TPB^{\ominus}] = 0$$

$$[29]\quad \frac{d[R^{\bullet}TPB^{\ominus}]}{dt} = k_{3a}[R^{\bullet}][TPB^{\ominus}] - (k_{-3a} + k_4[TPB^{\ominus}])[R^{\bullet}TPB^{\ominus}] = 0$$

Matrix summary:

$$[30]\quad \begin{bmatrix} -k_{-1} - k_{2a} & k_{-2a}[SO_3^{2\ominus}] & 0 \\ k_{2a} & -k_{-2a}[SO_3^{2\ominus}] - k_{3a}[TPB^{\ominus}] & k_{-3a} \\ 0 & k_{3a}[TPB^{\ominus}] & -k_{-3a} - k_4[TPB^{\ominus}] \end{bmatrix} \times \begin{bmatrix} [R^{\bullet}SO_3^{2\ominus}] \\ [R^{\bullet}] \\ [R^{\bullet}TPB^{\ominus}] \end{bmatrix} = \begin{bmatrix} -k_1[RSO_3^{\ominus}] \\ 0 \\ 0 \end{bmatrix}$$

Observed rate:

$$[31]\quad \frac{d[R^{\ominus}(TPB^{\ominus})_2]}{dt} = \frac{d[RSO_3^{\ominus}]}{dt} = k_{obs}[RSO_3^{\ominus}] = k_4[R^{\bullet}TPB^{\ominus}][TPB^{\ominus}]$$

Observed rate constant:

$$[32]\quad k_{obs} = \frac{k_4[R^{\bullet}TPB^{\ominus}][TPB^{\ominus}]}{[RSO_3^{\ominus}]}$$

$$[33]\quad k_{obs} = \{k_1k_{2a}k_{3a}k_4[TPB^{\ominus}]^2\} / \{k_{-1}k_{-2a}k_{-3a}[SO_3^{2\ominus}] + (k_{-1} + k_{2a})k_{3a}k_4[TPB^{\ominus}]^2 + k_{-1}k_{-2a}k_4[SO_3^{2\ominus}][TPB^{\ominus}]\} \qquad [8]$$

Scheme VI

$$[1]\quad RSO_3^{\ominus} \rightleftharpoons R^{\bullet}SO_3^{2\ominus}$$

$$[2b]\quad R^{\bullet}SO_3^{2\ominus} + TPB^{\ominus} \rightleftharpoons TPB^{\ominus}R^{\bullet}SO_3^{2\ominus}$$

$$[3b]\quad TPB^{\theta}R^{\bullet}SO_3^{2\theta} \rightleftharpoons R^{\bullet}TPB^{\theta} + SO_3^{2\theta}$$

$$[4]\quad R^{\bullet}TPB^{\theta} + TPB^{\theta} \longrightarrow R^{\bullet}(TPB^{\theta})_2$$

Steady state equations:

$$[34]\quad \frac{d[R^{\bullet}SO_3^{2\theta}]}{dt} = k_1[RSO_3^{\theta}] - (k_{-1} + k_{2b}[TPB^{\theta}])[R^{\bullet}SO_3^{2\theta}] + k_{-2b}[TPB^{\theta}R^{\bullet}SO_3^{2\theta}] = 0$$

$$[35]\quad \frac{d[TPB^{\theta}R^{\bullet}SO_3^{2\theta}]}{dt} = k_{2b}[R^{\bullet}SO_3^{2\theta}][TPB^{\theta}] - (k_{-2b} + k_{3b})[TPB^{\theta}R^{\bullet}SO_3^{2\theta}] + k_{-3b}[R^{\bullet}TPB^{\theta}][SO_3^{2\theta}] = 0$$

$$[36]\quad \frac{d[R^{\bullet}TPB^{\theta}]}{dt} = k_{3b}[TPB^{\theta}R^{\bullet}SO_3^{2\theta}] - (k_{-3b}[SO_3^{2\theta}] + k_4[TPB^{\theta}])[R^{\bullet}TPB^{\theta}] = 0$$

Matrix summary:

$$[37]\quad \begin{bmatrix} -k_{-1} - k_{2b}[TPB^{\theta}] & k_{-2b} & 0 \\ k_{2b}[TPB^{\theta}] & -k_{-2b} - k_{3b} & k_{-3b}[SO_3^{2\theta}] \\ 0 & k_{3b} & -k_{-3b}[SO_3^{2\theta}] - k_4[TPB^{\theta}] \end{bmatrix} \times \begin{bmatrix} [R^{\bullet}SO_3^{2\theta}] \\ [TPB^{\theta}R^{\bullet}SO_3^{2\theta}] \\ [R^{\bullet}TPB^{\theta}] \end{bmatrix} = \begin{bmatrix} -k_1[RSO_3^{\theta}] \\ 0 \\ 0 \end{bmatrix}$$

Observed rate:

$$[38]\quad \frac{d[R^{\bullet}(TPB^{\theta})_2]}{dt} = -\frac{d[RSO_3^{\theta}]}{dt} = k_{obs}[RSO_3^{\theta}]$$

$$= k_4[R^{\bullet}TPB^{\theta}][TPB^{\theta}]$$

Observed rate constant:

$$[39]\quad k_{obs} = \frac{k_4[R^{\bullet}TPB^{\theta}][TPB^{\theta}]}{[RSO_3^{\theta}]}$$

$$[40]\quad k_{obs} = (k_1 k_{2b} k_{3b} k_4 [TPB^{\theta}]^2) \,/\, (k_{-1}k_{-2b}k_{-3b}[SO_3^{2\theta}] + k_{-1}(k_{-2b} + k_{3b})k_4[TPB^{\theta}] + k_{2b}k_{3b}k_4[TPB^{\theta}]^2) \qquad [12]$$

Scheme VII

$$[1]\quad RSO_3^{\theta} \rightleftharpoons R^{\bullet}SO_3^{2\theta}$$

$$[2a]\quad R^{\bullet}SO_3^{2\theta} \rightleftharpoons R^{\bullet} + SO_3^{2\theta}$$

$$[3a]\quad R^{\bullet} + TPB^{\theta} \longrightarrow R^{\bullet}TPB^{\theta}$$

Steady state equations:

$$[41]\quad \frac{d[R^{\bullet}SO_3^{2\theta}]}{dt} = k_1[RSO_3^{\theta}] - (k_{-1} + k_{2a})[R^{\bullet}SO_3^{2\theta}] + k_{-2a}[R^{\bullet}][SO_3^{2\theta}] = 0$$

$$[42]\quad \frac{d[R^{\bullet}]}{dt} = k_{2a}[R^{\bullet}SO_3^{2\theta}] - (k_{-2a}[SO_3^{2\theta}] + k_{3a}[TPB^{\theta}])[R^{\bullet}] = 0$$

Matrix summary:

$$[43]\quad \begin{bmatrix} -k_{-1a} - k_{2a} & k_{-2a}[SO_3^{2\theta}] \\ k_{2a} & -k_{-2a}[SO_3^{2\theta}] - k_{3a}[TPB^{\theta}] \end{bmatrix} \times \begin{bmatrix} [R^{\bullet}SO_3^{2\theta}] \\ [R^{\bullet}] \end{bmatrix} = \begin{bmatrix} -k_1[RSO_3^{\theta}] \\ 0 \end{bmatrix}$$

Observed rate:

$$[44]\quad \frac{d[R^{\bullet}(TPB^{\theta})_2]}{dt} = -\frac{d[RSO_3^{\theta}]}{dt} = k_{obs}[RSO_3^{\theta}] = k_{3a}[R^{\bullet}][TPB^{\theta}]$$

Observed rate constant:

$$[45]\quad k_{obs} = \frac{k_{3a}[R^{\bullet}][TPB^{\theta}]}{[RSO_3^{\theta}]}$$

$$[46]\quad k_{obs} = \frac{k_1 k_{2a} k_{3a}[TPB^{\theta}]}{(k_{-1} + k_{2a})k_{3a}[TPB^{\theta}] + k_{-1}k_{-2a}[SO_3^{2\theta}]} \qquad [15]$$

Scheme VIII

$$[1]\quad RSO_3^{\theta} \rightleftharpoons R^{\bullet}SO_3^{2\theta}$$

$$[2b]\quad R^{\bullet}SO_3^{2\theta} + TPB^{\theta} \rightleftharpoons TPB^{\theta}R^{\bullet}SO_3^{2\theta}$$

$$[3b]\quad TPB^{\theta}R^{\bullet}SO_3^{2\theta} \longrightarrow R^{\bullet}TPB^{\theta} + SO_3^{2\theta}$$

Since this scheme is obviously incorrect, no expressions are derived.

Scheme IX

[1] $RSO_3^{\ominus} \rightleftharpoons R^{\bullet}SO_3^{2\ominus}$

[2a] $R^{\bullet}SO_3^{2\ominus} \rightleftharpoons R^{\bullet} + SO_3^{2\ominus}$

[2b] $R^{\bullet}SO_3^{2\ominus} + TPB^{\ominus} \rightleftharpoons TPB^{\ominus}R^{\bullet}SO_3^{2\ominus}$

[3a] $R^{\bullet} + TPB^{\ominus} \longrightarrow R^{\bullet}TPB^{\ominus}$

[3b] $TPB^{\ominus}R^{\bullet}SO_3^{2\ominus} \longrightarrow R^{\bullet}TPB^{\ominus} + SO_3^{2\ominus}$

Steady state equations:

$$[47]\quad \frac{d[R^{\bullet}SO_3^{2\ominus}]}{dt} = k_1[RSO_3^{\ominus}] - (k_{-1} + k_{2a} + k_{2b}[TPB^{\ominus}])[R^{\bullet}SO_3^{2\ominus}] + k_{-2a}[R^{\bullet}][SO_3^{2\ominus}] + k_{-2b}[TPB^{\ominus}R^{\bullet}SO_3^{2\ominus}] = 0$$

$$[48]\quad \frac{d[R^{\bullet}]}{dt} = k_{2a}[R^{\bullet}SO_3^{2\ominus}] - (k_{-2a}[SO_3^{2\ominus}] + k_{3a}[TPB^{\ominus}])[R^{\bullet}] = 0$$

$$[49]\quad \frac{d[TPB^{\ominus}R^{\bullet}SO_3^{2\ominus}]}{dt} = k_{2b}[R^{\bullet}SO_3^{2\ominus}][TPB^{\ominus}] - (k_{-2b} + k_{3b})[TPB^{\ominus}R^{\bullet}SO_3^{2\ominus}] = 0$$

Matrix summary:

$$[50]\quad \begin{bmatrix} -k_{-1} - k_{2a} - k_{2b}[TPB^{\ominus}] & k_{-2a}[SO_3^{2\ominus}] \\ k_{2a} & -k_{-2a}[SO_3^{2\ominus}] - k_{3a}[TPB^{\ominus}] \\ k_{2b}[TPB^{\ominus}] & 0 \end{bmatrix}$$

$$\begin{bmatrix} k_{-2b} \\ 0 \\ -k_{-2b} - k_{3b} \end{bmatrix} \times \begin{bmatrix} [R^{\oplus}SO_3^{2\ominus}] \\ [R^{\oplus}] \\ [TPB^{\ominus}R^{\oplus}SO_3^{2\ominus}] \end{bmatrix} = \begin{bmatrix} -k\,[RSO_3^{\ominus}] \\ 0 \\ 0 \end{bmatrix}$$

Observed rate:

$$[51] \quad \frac{d[R^{\oplus}(TPB^{\ominus})_2]}{dt} = -\frac{d[RSO_3^{\ominus}]}{dt} = k_{obs}[RSO_3^{\ominus}]$$

$$= k_{3a}[R^{\oplus}][TPB^{\ominus}] + k_{3b}[TPB^{\ominus}R^{\oplus}SO_3^{2\ominus}]$$

Observed rate constant:

$$[52] \quad k_{obs} = \frac{k_{3a}[R^{\oplus}][TPB^{\ominus}] + k_{3b}[TPB^{\ominus}R^{\oplus}SO_3^{2\ominus}]}{[RSO_3^{\ominus}]}$$

$$[53] \quad k_{obs} = \{k_1k_{2a}k_{3a}(k_{-2b} + k_{3b})[TPB^{\ominus}]$$
$$+ k_1k_{2b}k_{3b}(k_{-2a}[SO_3^{2\ominus}] + k_{3a}[TPB^{\ominus}])[TPB^{\ominus}]\} /$$
$$\{k_{-2a}k_{2b}k_{3b}[TPB^{\ominus}][SO_3^{2\ominus}]$$
$$+ (k_{-1} + k_{2a})(k_{-2b} + k_{3b})k_{3a}[TPB^{\ominus}]$$
$$+ k_{-1}k_{-2a}(k_{-2b} + k_{3b})[SO_3^{2\ominus}]$$
$$+ k_{2b}k_{3a}k_{3b}[TPB^{\ominus}]^2\} \qquad [18]$$

Scheme X

$$[1] \quad RSO_3^{\ominus} \rightleftharpoons R^{\oplus}SO_3^{2\ominus}$$

$$[2a] \quad R^{\oplus}SO_3^{2\ominus} \rightleftharpoons R^{\oplus} + SO_3^{2\ominus}$$

$$[3a] \quad R^{\oplus} + TPB^{\ominus} \longrightarrow R^{\oplus}TPB^{\ominus}$$

$$[2b3b] \quad R^{\oplus}SO_3^{2\ominus} + TPB^{\ominus} \longrightarrow R^{\oplus}TPB^{\ominus} + SO_3^{2\ominus}$$

Steady state equations:

$$[54]\quad \frac{d[R^{\bullet}SO_3^{2\ominus}]}{dt} = k_1[RSO_3^{\ominus}] - (k_{-1} + k_{2a} + k_{2b3b}[TPB^{\ominus}])[R^{\bullet}SO_3^{2\ominus}] + k_{-2a}[R^{\bullet}][SO_3^{2\ominus}] = 0$$

$$[55]\quad \frac{d[R^{\bullet}]}{dt} = k_{2a}[R^{\bullet}SO_3^{2\ominus}] - (k_{-2a}[SO_3^{2\ominus}] + k_{3a}[TPB^{\ominus}])[R^{\bullet}] = 0$$

Matrix summary:

$$[56]\quad \begin{bmatrix} -k_{-1} - k_{2a} - k_{2b3b}[TPB^{\ominus}] & k_{-2a}[SO_3^{2\ominus}] \\ k_{2a} & -k_{-2a}[SO_3^{2\ominus}] - k_{3a}[TPB^{\ominus}] \end{bmatrix} \times \begin{bmatrix} [R^{\bullet}SO_3^{2\ominus}] \\ [R^{\bullet}] \end{bmatrix} = \begin{bmatrix} -k_1[RSO_3^{\ominus}] \\ 0 \end{bmatrix}$$

Observed rate:

$$[57]\quad \frac{d[R^{\bullet}(TPB^{\ominus})_2]}{dt} = -\frac{d[RSO_3^{\ominus}]}{dt} = k_{obs}[RSO_3^{\ominus}] = k_{3a}[R^{\bullet}][TPB^{\ominus}] + k_{2b3b}[R^{\bullet}SO_3^{2\ominus}][TPB^{\ominus}]$$

Observed rate constant:

$$[58]\quad k_{obs} = \frac{(k_{3a}[R^{\bullet}] + k_{2b3b}[R^{\bullet}SO_3^{2\ominus}])[TPB^{\ominus}]}{[RSO_3^{\ominus}]}$$

$$[59] \quad k_{obs} = \{k_1 k_{-2a} k_{2b3b} [TPB^{\theta}][SO_3^{2\theta}] + k_1 k_{2b3b} k_{3a} [TPB^{\theta}]^2 + k_1 k_{2a} k_{3a} [TPB^{\theta}]\} / \{k_{-1} k_{-2a} [SO_3^{2\theta}] + (k_{-1} + k_{2a}) k_{3a} [TPB^{\theta}] + k_{-2a} k_{2b3b} [TPB^{\theta}][SO_3^{2\theta}] + k_{2b3b} k_{3a} [TPB^{\theta}]^2\} \quad [22]$$

Appendix C

Figures 29 and 30 are a summary of the results. The lines are calculated by Equation [26] from the parameters given in Table 27, page 86, and the concentrations used. Equation [26] is the derived expression for the pseudo-first order rate constant.

Figures 31 and 32 show the correlation between the observed rate constants and the calculated rate constants. The calculated rate constants were also derived by Equation [26] using the parameters in Table 27 and the concentrations used. The plots indicate the correlation to cluster well around the line through the origin of unity slope. Thus, the data are well fitted to Equation [26] by the parameters in Table 27.

Reaction of $pMeOMGSO_3^{\ominus}$ with $TPB^{\ominus}$

Summary Plots

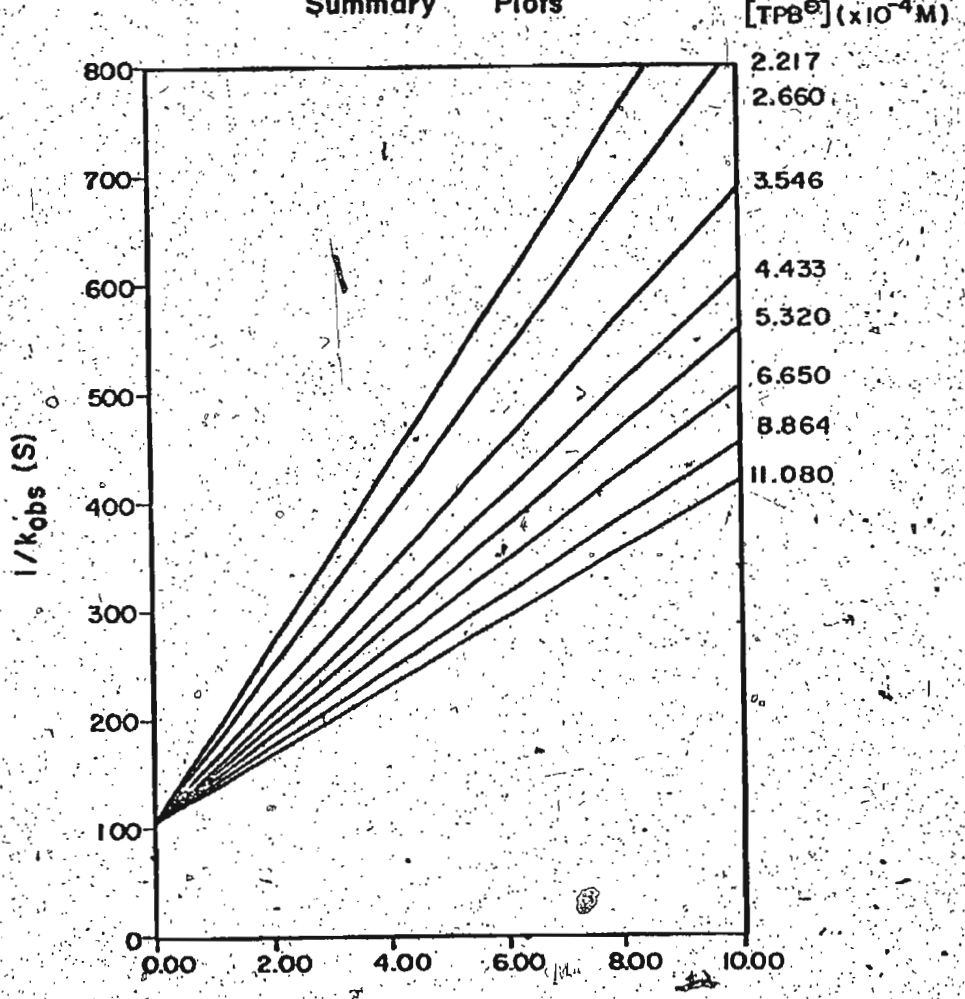

Fig. 29

Reaction of $MGSO_3^{\ominus}$ with $TPB^{\ominus}$

Summary plots

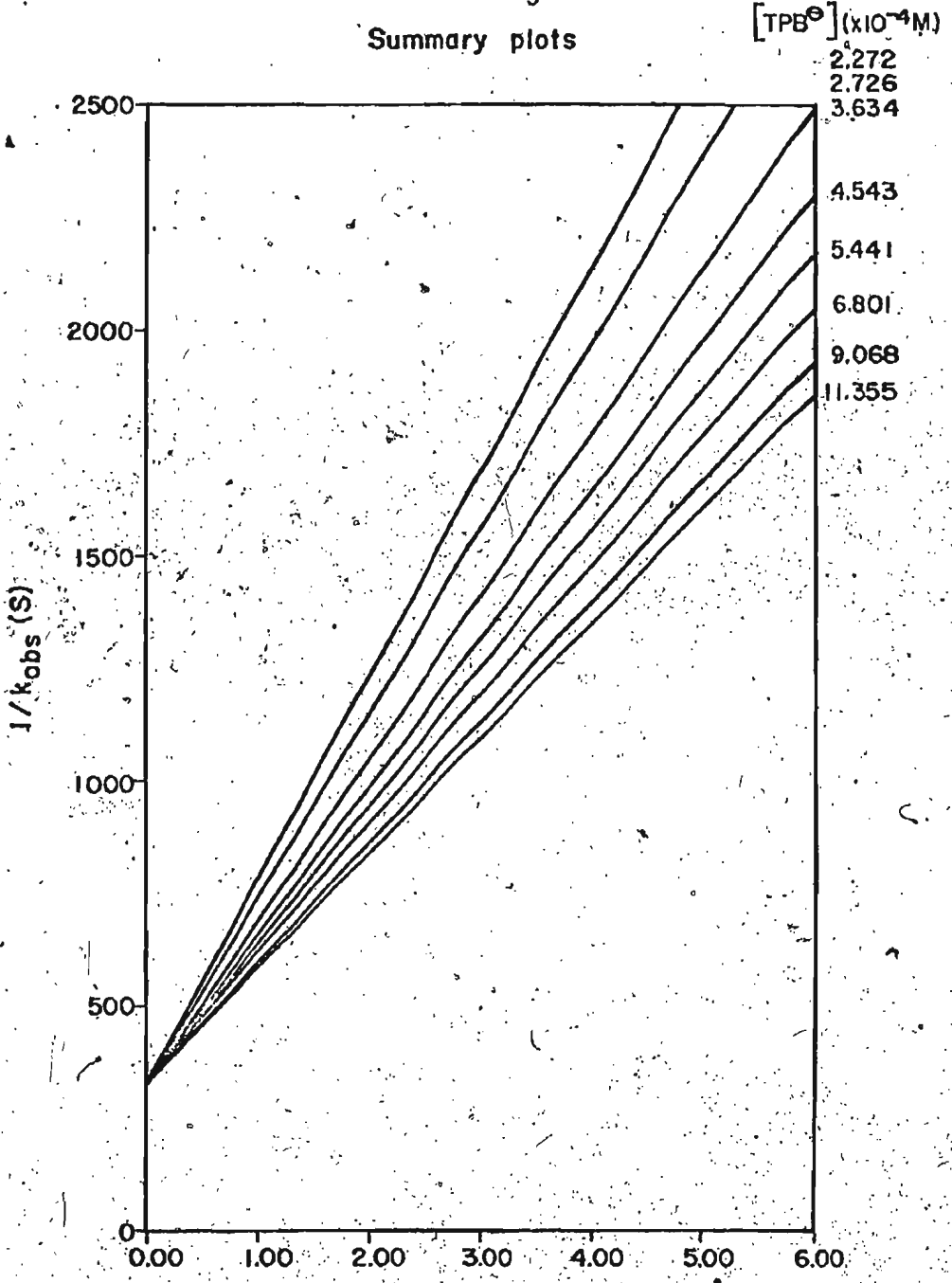

Fig. 30

Reaction of $pMeOMGSO^{\ominus}$ with $TPB^{\ominus}$

k_{calc} —vs— k_{obs}

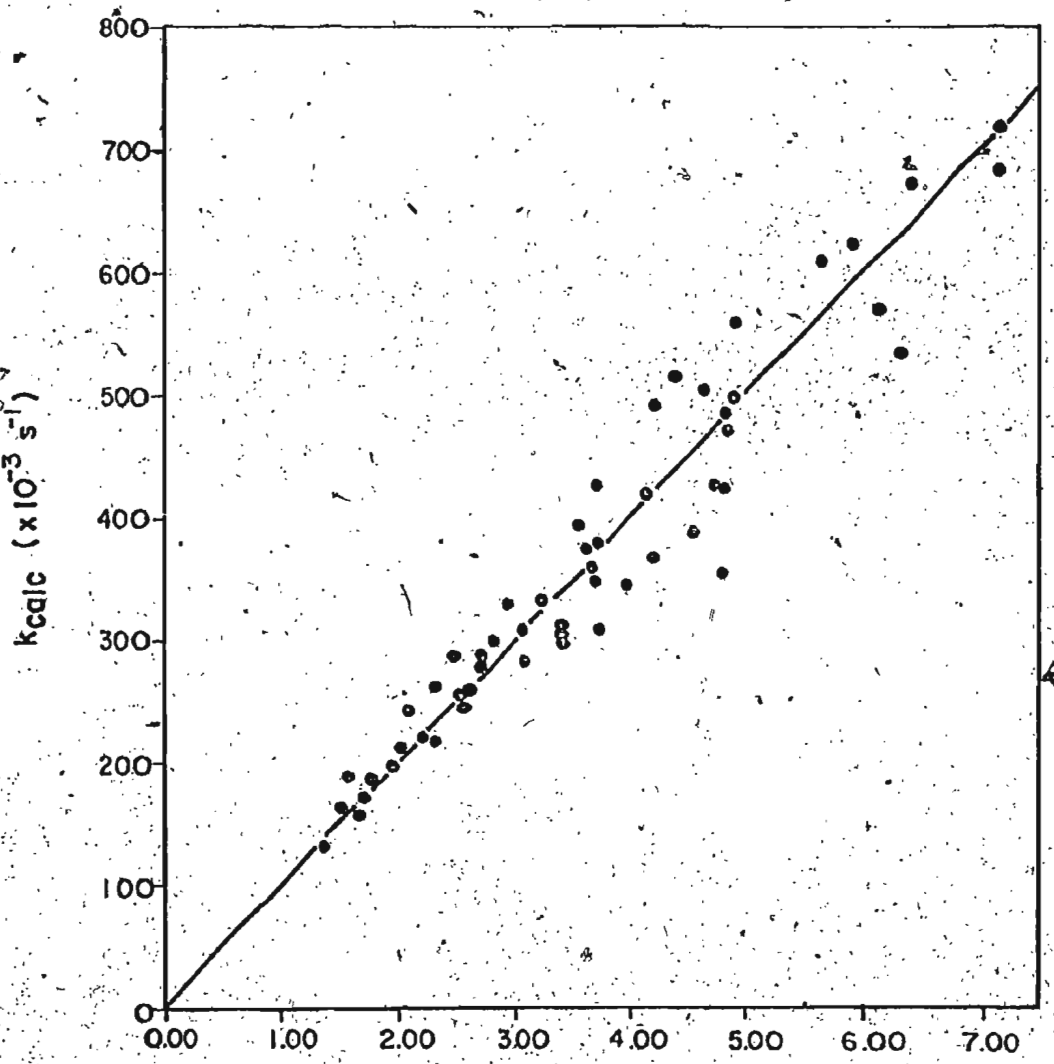

Fig. 31

Reaction of $MGSO_3^{\ominus}$ with $TPB^{\ominus}$

k_{calc} -vs- k_{obs}

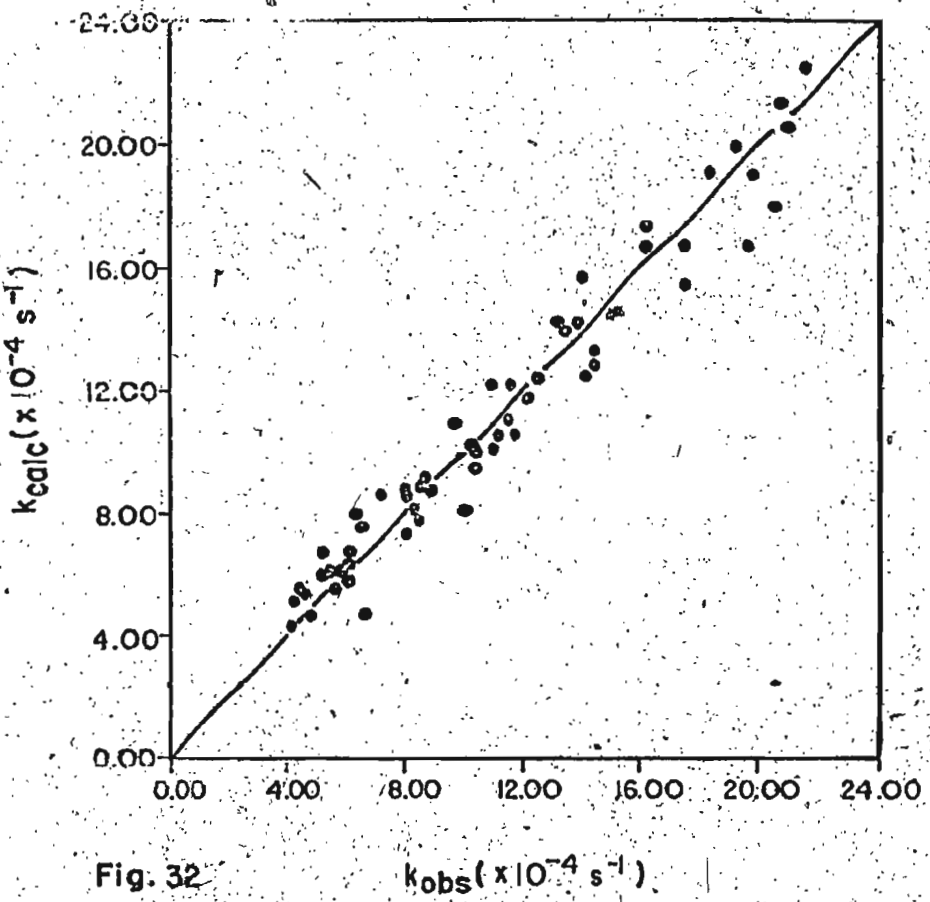

Fig. 32

References

1. C.K. Ingold. Structure and mechanism in organic chemistry. Cornell University Press, Ithaca, N.Y. 1953. Chap. 7.
2. D.J. McLennan. Acc. Chem. Res. 9, 281(1976) and references therein.
3. M.L. Bird, E.D. Hughes, and C.K. Ingold. J. Chem. Soc. 634(1954).
4. V. Gold. J. Chem. Soc. 4633(1956).
5. S. Winstein, P.E. Klinedist, Jr., and G.C. Robinson. J. Am. Chem. Soc. 83, 885(1961).
6. S. Winstein, P.E. Klinedist, Jr., and E. Clippinger. J. Am. Chem. Soc. 83, 4986(1961).
7. S. Winstein, R. Baker, and S.G. Smith. J. Am. Chem. Soc. 86, 2072(1964).
8. E.A. Moelwyn-Hughes. The kinetics of reactions in solution. Clarendon Press, Oxford, England. 1947. Chap. I p. 16.
9. R.A. Sneen and J.W. Larsen. J. Am. Chem. Soc. 91, 362 (1969).
10. R.A. Sneen and J.W. Larsen. J. Am. Chem. Soc. 91, 6031 (1969).
11. R.A. Sneen. Acc. Chem. Res. 6, 46(1970).
12. J.M.W. Scott. Can. J. Chem. 48, 3807(1970).
13. R.E. Robertson, A. Annesa, and J.M.W. Scott. Can. J. Chem. 53, 3106(1975).

14. J.C. Turgeon and V.K. LaMer. J. Am. Chem. Soc. 74, 5988 (1952).

15. C.G. Swain and C.B. Scott. J. Am. Chem. Soc. 75, 141 (1953).

16. J.A. Hirsch. Concepts in theoretical organic chemistry. Allyn and Bacon, Boston, Mass. 1975., Chap. 7.

17. C.D. Ritchie. Acc. Chem. Res. 5, 348(1972).

18. G.S. Hammond. J. Am. Chem. Soc. 77, 334(1955).

19. J.E. Dixon and T.C. Bruice. J. Am. Chem. Soc. 93, 3248 (1971).

20. S.J. Collens. Some reactions of crystal violet, Honours Thesis, Memorial University of Newfoundland, 1978.

21. K.H. Hillier, J.M.W. Scott, D.J. Barnes, and F.J.P. Steele. Can. J. Chem. 54, 3312(1976).

22. Addy Pross. J. Am. Chem. Soc. 98, 776(1976).

23. H.H. Freedman. Carbonium ions, Vol. IV. edited by George A. Olah and Paul von R. Schleyer. Wiley Interscience, Toronto, Ontario. 1973. Chap. 28.

24. Arthur I. Vogel. Quantitative inorganic analysis, third edition. Longman, London, England. 1961.

25. P. Moore. J. Chem. Soc. Faraday Trans. I. 68, 1890 (1972).

26. S.H. Morris, J.M.W. Scott, and F. Steele. Can. J. Chem. 55, 686(1977).

27. W.E. Wentworth. J. Chem. Ed. 42, 96(1965).

28. C.D. Ritchie and P.O.I. Virtanen. J. Am. Chem. Soc. 95, 1882(1973).

29. Clifford A. Bunton and Sung K. Huang. J. Am. Chem. Soc. 96, 515(1974).